

MMSE PER-SUBCHANNEL EQUALISATION AND CHANNEL ESTIMATION FOR FBMC

A Project Report

submitted by

YESWANTH REDDY.G

*in partial fulfilment of the requirements
for the award of the degree of*

BACHELOR OF TECHNOLOGY



**DEPARTMENT OF ELECTRICAL ENGINEERING
INDIAN INSTITUTE OF TECHNOLOGY MADRAS.**

June 2016

THESIS CERTIFICATE

This is to certify that the thesis titled **MMSE PER-SUBCHANNEL EQUALISATION AND CHANNEL ESTIMATION FOR FBMC**, submitted by **Yeswanth Reddy.G**, to the Indian Institute of Technology, Madras, for the award of the degree of **Bachelor of Technology**, is a bona fide record of the research work done by him under our supervision. The contents of this thesis, in full or in parts, have not been submitted to any other Institute or University for the award of any degree or diploma.

Prof. 1
Research Guide
Professor David Koilpillai
Dept. of Electrical Engineering
IIT-Madras, 600 036

Place: Chennai

Date: 15th June 2016.

ACKNOWLEDGEMENTS

Thanks to Prof. David Koilpillai for his continued guidance and Sai pavan kumar(EE11B117)
,Venkata Subba reddy(EE14M017) for their help in finishing this project.

ABSTRACT

The following paper details the structure of FBMC system and it's polyphase implementation. Per-sub channel MMSE equaliser is discussed and equalizer coefficients are derived. The performance of two channel estimation methods , IAM and POP are compared. The effect of Carrier frequency Offset is seen and methods to estimate, compensate CFO are discussed.

TABLE OF CONTENTS

ACKNOWLEDGEMENTS	i
ABSTRACT	ii
LIST OF TABLES	v
LIST OF FIGURES	vi
1 FBMC	vii
1.1 Structure of Filter Bank-based Multicarrier system	vii
1.2 Prototype filter design	ix
1.3 OQAM modulation	xi
1.4 Polyphase Implementation of FBMC	xiii
1.4.1 Synthesis Filter	xiii
1.4.2 Analysis filter	xvi
1.5 BER for FBMC under AWGN channel	xix
1.5.1 BER for OFDM	xix
1.5.2 BER for FBMC	xix
2 MMSE Per-subchannel Equalizer	xxi
2.1 Introduction	xxi
2.2 Derivation of MMSE Equalizer co-efficients	xxiii
2.3 Simulation of MMSE Equalisation	xxv
2.4 Two-stage MMSE	xxviii
3 Channel estimation	xxx
3.1 Channel model	xxx
3.2 Interference Approximation method(IAM)	xxxiii
3.3 Pair of Pilots scheme(POP)	xxxiv
3.4 Simulation results using channel estimation	xxxvii

4	Carrier Frequency Offset(CFO)	xxxix
4.1	Effect of CFO on Equalization	xxxix
4.2	Estimation of CFO	xl
4.3	Compensation of CFO	xlii
4.4	CFO simulations	xliii

LIST OF TABLES

1.1	Impulse response of the transmitter-receiver cascade of filter bank transmission system at $K = 4$	xiii
3.1	Impulse response of the filter bank transmission system w.r.t $x_{k,n}$ at $\mathbf{K} = 4$	xxxi
3.2	OQAM/IAM	xxxvii
3.3	OQAM/POP	xxxvii

LIST OF FIGURES

1.1	FBMC TMUX configuration	vii
1.2	OQAM preprocessing	viii
1.3	OQAM post-processing	ix
1.4	Impulse and frequency response of prototype filter for K=4 and M=256	x
1.5	A section of filter bank for K=4	xi
1.6	Symbol mapping for QAM and OQAM modulation	xii
1.7	Synthesis filter bank	xv
1.8	Analysis filter bank	xvii
1.9	Analysis filter bank-DFT mode	xviii
1.10	Bit Error Rate vs Eb/N0 for FBMC simulation under AWGN	xx
2.1	FBMC system overview	xxi
2.2	Sub carrier model for FBMC	xxii
2.3	Desired OQAM impulse response	xxii
2.4	Comparision of FBMC with CP-OFDM	xxvi
2.5	Comparision of MMSE Equalisation with M=256 and different taps	xxvii
2.6	Two stage MMSE Equalisation with M=256 and 6 taps	xxix
3.1	MMSE Equalisation with channel estimation (4-QAM,M=256,N=6)	xxxviii
4.1	Sub-channel frequency response and distortion due to CFO = 0.25 .	xl
4.2	Sub-channel frequency response distortion due to CFO = 0.01,0.05,0.1,0.2.	xli
4.3	Receiver model for sub-channel in presence of CFO with CFO compen- sation and equalisation showing the actual model and equivalent model for MMSE	xliii
4.4	MAX error(-o) and RMS error(-x) while estimating CFO for $E_b/N_0 =$ 5, 20, 30	xliv
4.5	BER comparision for $E_b/N_0 = 20$ with CFO estimated and amplitude distortion,phase distortion corrections	xl v
4.6	BER comparision for $E_b/N_0 = 30$ with CFO estimated and amplitude distortion,phase distortion corrections	xl v

CHAPTER 1

FBMC

1.1 Structure of Filter Bank-based Multicarrier system

The synthesis and analysis filters form an important part of the FBMC system. M different signals are multiplexed in time and sent through different sub-bands formed by the synthesis-analysis cascade. The design objective for these filters is zero ISI and minimising the out-of-band leakage.

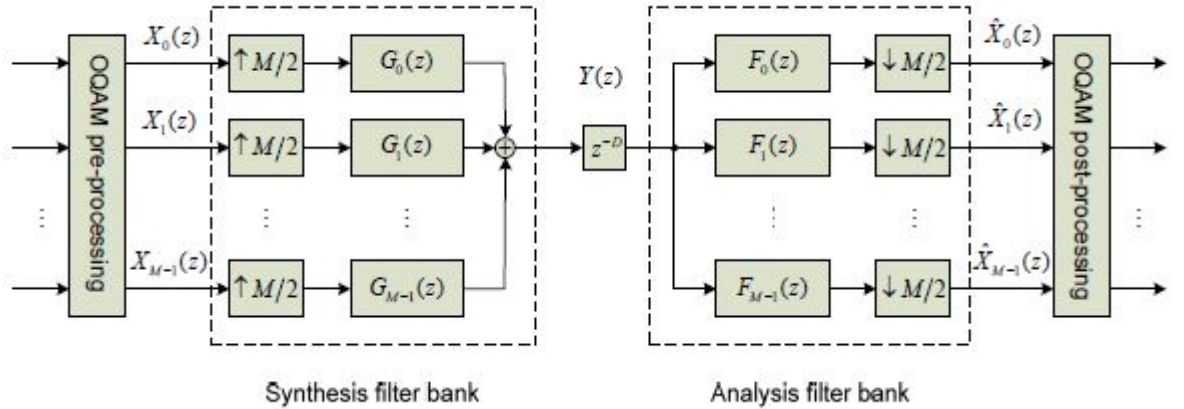


Figure 1.1: FBMC TMUX configuration

Fig. 1.1 shows a delay D in the system situated between synthesis and analysis filter. This delay should be such that it ensures the position of the centre tap of the convolution of k^{th} synthesis and analysis filter at an integer multiple of $M/2$.

$$L_p = KM + 1 - D \quad (1.1)$$

i.e for example when $L_p = KM$, $D = 1$.

The input signal to the synthesis filters are upsampled by $M/2$ instead of M as in typical multiplexing. The individual signals can be recovered in spite of the overlap due to the way in which OQAM pre-processing and post processing is done as shown in the Fig. 1.2

For each sub carrier, OQAM pre-processing first separates real,imaginary parts of the input and transmits them serially. Thus OQAM processing increases the sampling rate by a factor of 2. Then the sequence is multiplied by $\theta_{k,n}$ which is either j or 1 . The samples $x'_k[n]$ are either purely real or imaginary.

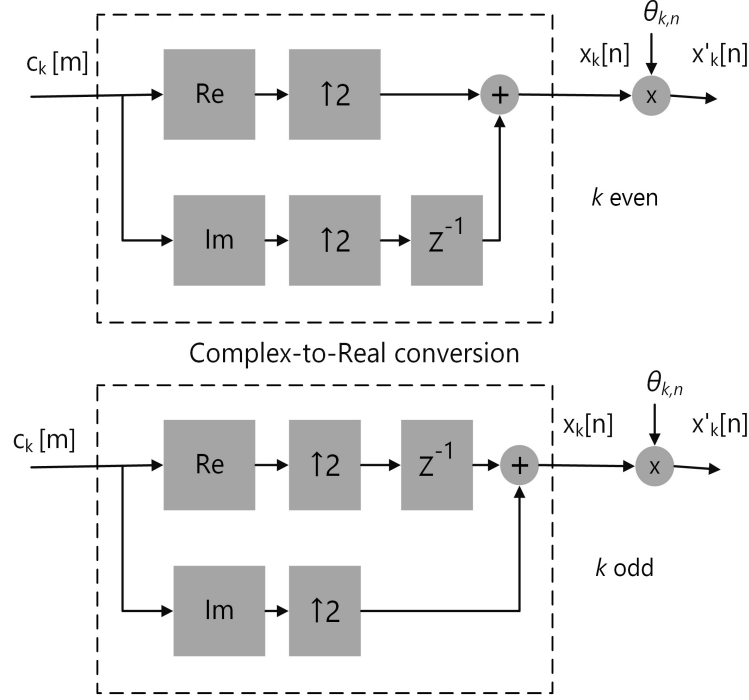


Figure 1.2: OQAM preprocessing

The pattern of real and imaginary samples and the sequence $\theta_{k,n}$ depend on whether sub-carrier is even or odd.

The sequence $\theta_{k,n}$ is given by:

$$\theta_{k,n} = \begin{cases} 1, j, 1, j, 1, j, \dots & \text{when } k \text{ is even} \\ j, 1, j, 1, j, 1, \dots & \text{when } k \text{ is odd} \end{cases}$$

Similarly in OQAM post-processing block when we receive the OQAM symbols, we first multiply them by $\theta_{k,n}^*$ and take the real part to get sequence equivalent to $x_{k,n}$. We then combine this real sequence in pairs to get a complex symbol as shown in the figure. Again the order in which they are combined depends on k .

The Principle used to transmit in filter bank based systems is shown in the figures above. The filters used for different carriers are frequency shifted versions of a single

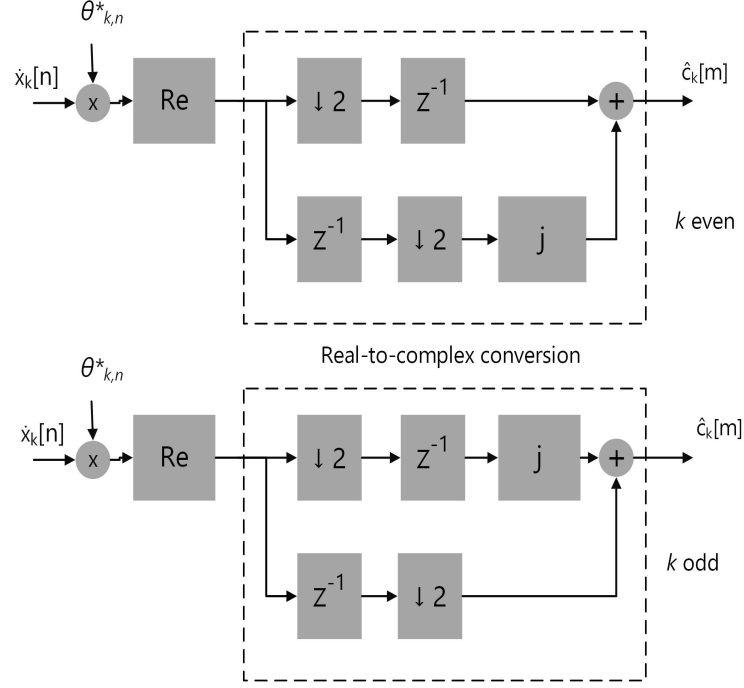


Figure 1.3: OQAM post-processing

filter associated with zero frequency carrier termed as prototype filter. Prototype filters are characterised by the overlapping factor K , which is the ratio of impulse response duration to the multicarrier symbol period T i.e it is the number of multicarrier symbols which overlap in time domain. In frequency domain it is the number of coefficients within the sub-carrier spacing $1/M$.

1.2 Prototype filter design

The filter used to transmit the data must satisfy Nyquist criterion to avoid Intersymbol interference i.e the impulse response of the filter must be zero at all the integer multiples of the symbol period T . In frequency domain this corresponds to symmetry condition over cutoff frequency $f_{sym}/2$ i.e the frequency response must satisfy the following equation-

$$\frac{1}{T} \sum_{k=-\infty}^{k=+\infty} S(f + k/T) = 1 \quad (1.2)$$

Then we can design a Nyquist filter by considering the frequency coefficients and imposing the symmetry condition. In transmission systems, the Nyquist filter is divided

into two parts ,half at the transmitter and other half at receiver. So the symmetry condition is satisfied by the squares of the frequency coefficients of the half nyquist filters.

Let M be the number of sub carriers. Then the length of prototype filter $L = KM$. In frequency domain the filter response contains $2K - 1$ pulses.

Considering $K = 4$ we get

$$P_0 = 1$$

$$P_1 = 0.971960 = P_{-1}$$

$$P_2 = 1/\sqrt{2} = P_{-2}$$

$$P_3 = \sqrt{1 - P_1^2} = 0.235147 = P_{-3}$$

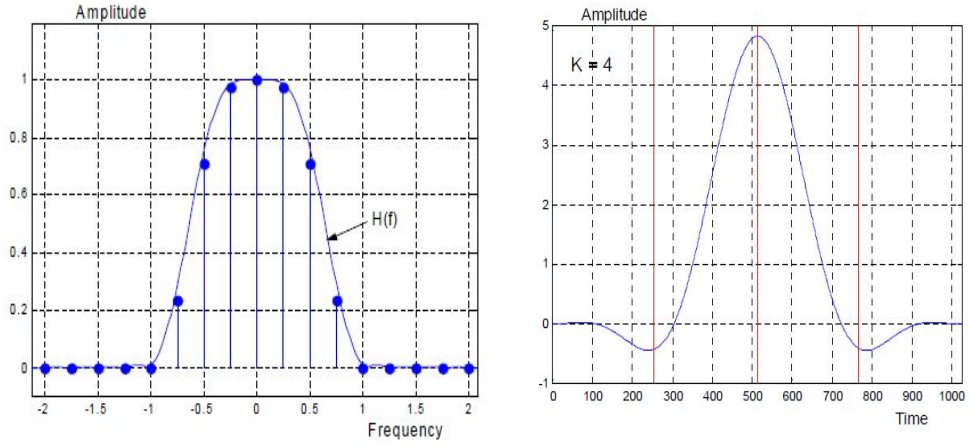


Figure 1.4: Impulse and frequency response of prototype filter for $K=4$ and $M=256$

They satisfy the equation

$$\frac{1}{K} \sum_{k=-(K-1)}^{K-1} |P_k|^2 = 1. \quad (1.3)$$

The continuous frequency response is obtained from the above coefficients through sinc interpolation which gives

$$P(f) = \sum_{k=-(K-1)}^{(K-1)} P_k \frac{\sin(\pi(f - \frac{k}{MK})MK)}{MK \sin(\pi(f - \frac{k}{MK}))}$$

The impulse response $p(t)$ in time is given by the following equation

$$p(t) = 1 + 2 \sum_{k=1}^{K-1} P_k \cos(2\pi \frac{kt}{KT}) \quad (1.4)$$

The remaining filters are obtained by frequency shifting the prototype filter. The filter of k^{th} sub carrier is obtained by multiplying prototype filter coefficients by $e^{j2\pi km/M}$.

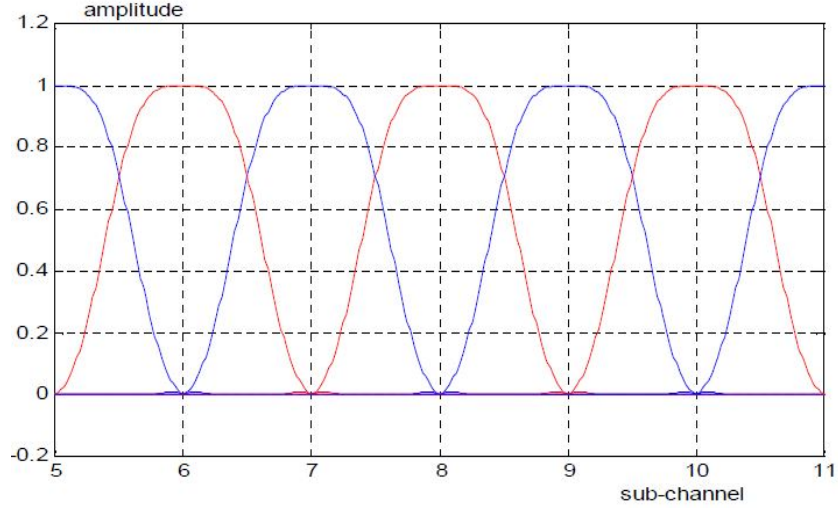


Figure 1.5: A section of filter bank for K=4

The figure above shows the filter bank system for $K = 4$. While considering the value of K it is important to note its effect on the side lobes. As seen in the figure above, with $K = 4$ the out of band ripples almost disappear and a given sub carrier filter only overlaps with its two adjacent filters in the filter bank. This as we will see later, is an important attribute responsible for using OQAM modulation in FBMC.

1.3 OQAM modulation

As it can be seen in Fig. 1.5 the interference in any given sub channel is due to the adjacent two sub carriers, the frequency response of inter sub channel interference is simplified. The interference due to an adjacent filter is given by the filter coefficients

$$I_k = P_k P_{K-k} \quad k = 1, 2, \dots, K-1.$$

The set of co-efficients are symmetrical for $K = 4$

$$I_1 = 0.228553 = I_3; I_2 = 0.5$$

In time domain, the impulse response of interference filter is given by

$$i(t) = [I_2 + 2I_1 \cos(2\pi \frac{t}{KT})] e^{j2\pi \frac{t}{2T}} \quad (1.5)$$

The factor $e^{j2\pi t/2T} = \cos(\pi t/T) + j \sin(\pi t/T)$ is the result of symmetry in coefficients of frequency response. You can see that the imaginary part of the interference from the adjacent channel is zero at integer multiples of symbol period T while the real part equals zero at odd multiples of $T/2$. The zero crossings are interleaved and this forms the basis of OQAM modulation.

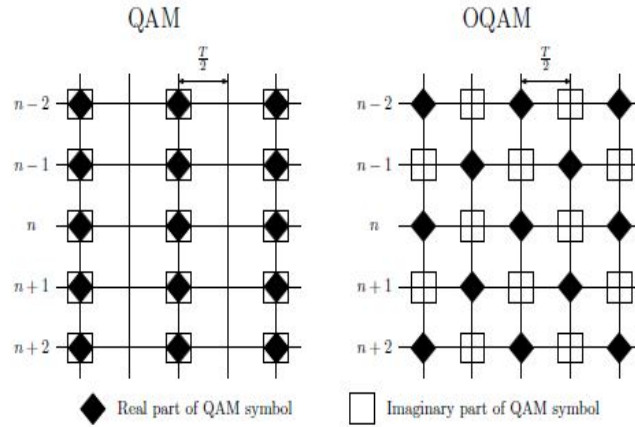


Figure 1.6: Symbol mapping for QAM and OQAM modulation

- As the adjacent sub channels overlap, orthogonality is needed. This is obtained by transmitting real and imaginary parts alternatively through adjacent subchannels at any given time. But this results in decrease of throughput by factor of 2.
- To restore the full capacity of the transmission system we exploit the fact that the zero crossings of real and imaginary part of interference are interleaved.

Then to reach full capacity double the sample rate of each subchannel and send in real and imaginary parts of iFFT alternatively in time separated by half the symbol duration.

Observe from Fig. 1.6 that at any time instant (denoted by horizontal axes) the data in adjacent subcarriers is orthogonal, thus can be retrieved inspite of interference from the adjacent sub-channel.

In fig 1.6 choose an OQAM symbol say at n and $t = T$

- Consider the interference caused by the real symbol, we see that the imaginary part of the interference is of no consequence at $(m + \frac{1}{2})T$ in adjacent sub-carriers. Now the real part of interference comes from the real part of interference filter response which as you can see from Eq. 1.5 is zero at odd multiples of $T/2$.
- Interference at mT and $n - 1$ due to the real symbol is purely real and thus the imaginary OQAM symbol can be recovered in post-processing.

The above statements becomes clearer when you take a look the impulse response of the transmitter - receiver cascade.

↓ subch,time→	n-4	n-3	n-2	n-1	n	n+1	n+2	n+3	n+4
k-1	0.005	j 0.043	-0.125	-j0.206	0.239	j 0.206	-0.125	-j0.043	0.005
k	0	-0.067	0	0.564	1	0.564	0	-0.067	0
k+1	0.005	j 0.043	-0.125	-j0.206	0.239	j 0.206	-0.125	-j0.043	0.005

Table 1.1: Impulse response of the transmitter-receiver cascade of filter bank transmission system at $K = 4$

1.4 Polyphase Implementation of FBMC

As you can see in Fig. 1.1 the TMUX filterbank model, upsampling takes place before any processing occurs on the input data which provides a possibility to apply noble identities of multi-rate signal processing. This paired with the fact that all the filters are frequency shifted versions can be used to reduce the computational complexity of the system by using polyphase structure.

1.4.1 Synthesis Filter

Since the synthesis filters are frequency shifted versions of prototype filter. We have :

$$g_k[m] = p[m] \exp(j \frac{2\pi k}{M} (m - \frac{L_p - 1}{2})) \quad (1.6)$$

This equation results in causal sub-carrier filters with impulse responses delayed by $\frac{L_p-1}{2}$ samples. The exponential part can be further simplified as follows :

$$\begin{aligned}
e_{k,m} &= \exp(j \frac{2\pi k}{M} (m - \frac{L_p-1}{2})) \\
&= \exp(-j \frac{2\pi k}{M} (\frac{L_p-1}{2})) \exp(j \frac{2\pi k m}{M}) \\
&= \beta_k \Theta_{k,m}
\end{aligned}$$

It can be seen that period of $e_{k,m}$ is M as $\Theta_{k,q+tM} = \Theta_{k,q}$ where $q = 0, 1, \dots, M-1$ and $t = 0, 1, \dots, K-1$. Now the k^{th} synthesis filter can be expressed in the form of type-1 polyphase filters as follows

$$\begin{aligned}
G_k(z) &= \sum_{m=0}^{L_p-1} p[m] e_{k,m} z^{-m} \\
&= \sum_{q=0}^{M-1} \sum_{t=0}^{K-1} g[q+tM] \beta_k \Theta_{k,q+tM} z^{-(q+tM)} \\
&= \sum_{q=0}^{M-1} \beta_k \Theta_{k,q} z^{-q} \sum_{t=0}^{K-1} g[q+tM] z^{-tM} \\
&= \sum_{q=0}^{M-1} \beta_k \Theta_{k,q} z^{-q} A_q(z^M)
\end{aligned}$$

Now the synthesis filter bank can be represented by the following matrix notation.

$$\mathbf{G}(z) = \mathbf{B} \cdot \mathbf{W} \cdot \mathbf{A}(z^M) \cdot \mathbf{c}(z), \quad (1.7)$$

where

$$\begin{aligned}
\mathbf{G}(z) &= [G_0(z) \ G_1(z) \dots G_{M-1}(z)]^T, \\
\mathbf{B} &= \text{diag}[\beta_0 \ \beta_1 \dots \beta_{M-1}], \\
[\mathbf{W}]_{k,q} &= \Theta_{k,q}, \\
\mathbf{A}(z^M) &= \text{diag}[A_0(z^M) \ A_1(z^M) \dots A_{M-1}(z^M)], \\
\mathbf{c}(z) &= [1 \ z^{-1} \dots z^{-(M-1)}]^T.
\end{aligned}$$

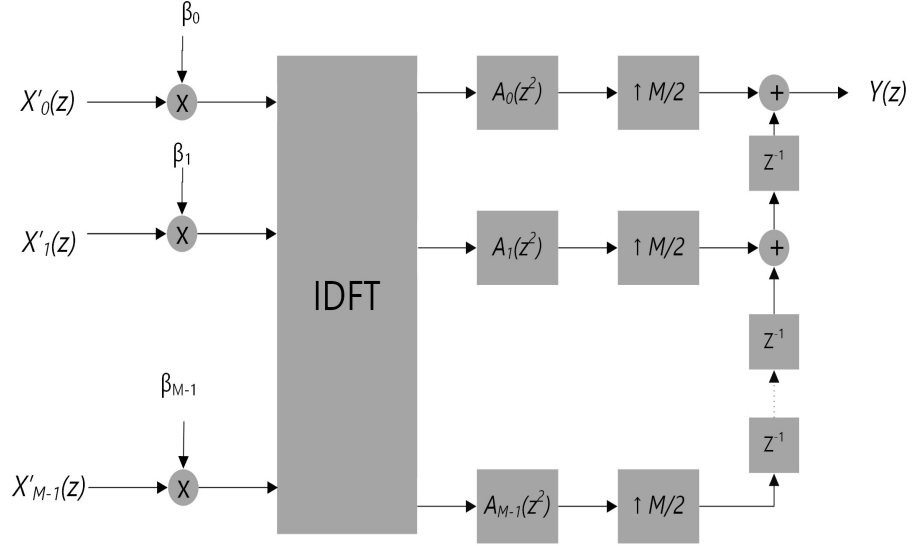


Figure 1.7: Synthesis filter bank

From the above equations and Fig. 1.1 we can see that the output signals before down-sampling can be written using matrix notation as

$$\begin{aligned}
 Y(z) &= \mathbf{G}^T(z) \cdot \mathbf{X}(z^{M/2}) \\
 &= (\mathbf{B} \cdot \mathbf{W} \cdot \mathbf{A}(z^M) \cdot \mathbf{c}(z))^T \cdot \mathbf{X}(z^{M/2}),
 \end{aligned}$$

where $\mathbf{X}(z^{M/2}) = [X_0(z^{M/2}) \ X_1(z^{M/2}) \dots X_{M-1}(z^{M/2})]^T$ and other matrices are from Eq. 1.7. The above equation can be interpreted in a way that the synthesis filter bank consists of upsamplers by $M/2, \beta_k$ -multipliers, IDFT, type-1 polyphase filters $A_q(z^M)$, and delay chain. Using well known multirate identity (PP. Vaidyanathan (1993)), all upsamplers can be moved through β_k -multipliers, IDFT, and polyphase filters. The final structure after modifying Fig. 1.1 as per all the above equations and shifting upsamplers is shown in Fig. 1.7.

1.4.2 Analysis filter

The k^{th} analysis filter is complex conjugated and time shifted version of corresponding synthesis filter .

$$\begin{aligned}
 f_k(m) &= g_k^*[L_p - 1 - m] \\
 &= p[L_p - 1 - m] \exp(-j \frac{2\pi k}{M} (L_p - 1 - m - \frac{L_p - 1}{2})) \\
 &= p[m] \exp(j \frac{2\pi k}{M} (m - \frac{L_p - 1}{2}))
 \end{aligned} \tag{1.8}$$

Therefore the z transform of the analysis filter can be represented as :

$$\begin{aligned}
 F_k(z) &= \sum_{m=0}^{L_p-1} f[m] e_{k,m} z^{-m} \\
 &= \sum_{q=0}^{M-1} \beta_k \Theta_{k,q} z^{-q} A_q(z^M).
 \end{aligned}$$

Moreover,all the analysis filters can be written using the matrix notation as follows.

$$\mathbf{F}(z) = \mathbf{B} \cdot \mathbf{W} \cdot \mathbf{A}(z^M) \cdot \mathbf{c}(z), \tag{1.9}$$

where

$$\mathbf{F}(z) = [F_0(z) \ F_1(z) \dots F_{M-1}(z)]^T \tag{1.10}$$

Now referring back to the original direct form representation in fig. 1.1 it can be seen that the output before the post processing can be written in matrix form as

$$\begin{aligned}
 \dot{\mathbf{X}}(z^{M/2}) &= \mathbf{F}(z^M) \cdot Y(z) \\
 &= \mathbf{B} \cdot \mathbf{W} \cdot \mathbf{A}(z^M) \cdot \mathbf{c}(z) \cdot Y(z)
 \end{aligned} \tag{1.11}$$

where $\dot{\mathbf{X}}(z^{M/2}) = [\dot{X}_0(z^{M/2}) \ \dot{X}_1(z^{M/2}) \dots \dot{X}_{M-1}(z^{M/2})]^T$ and other matrices are the same as from Eq. 1.7. The analysis filter has delay chain, type-1 polyphase filters, IDFT, β_k multipliers and downsamplers of $M/2$. The downsamplers can pass through the β_k multipliers, IDFT, type-1 polyphase filters yielding the structure shown -

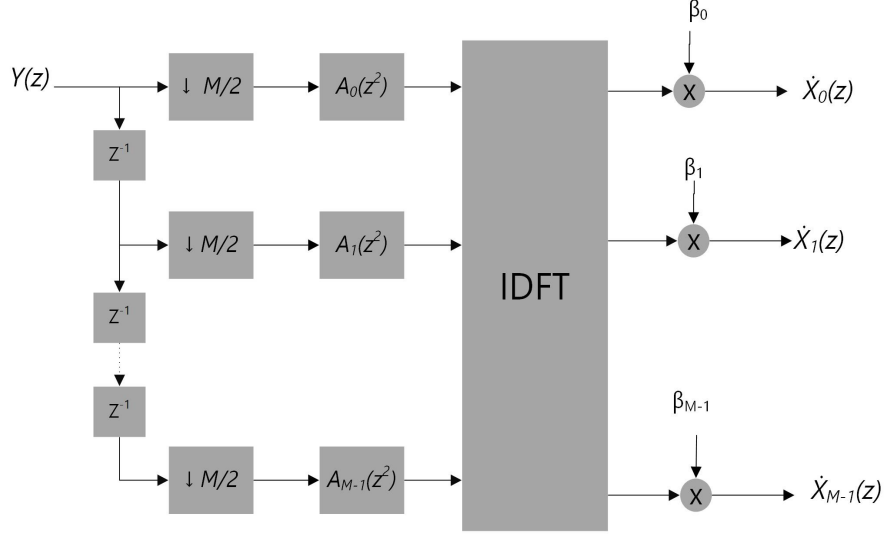


Figure 1.8: Analysis filter bank

It can be seen from the polyphase structure of analysis filter bank above ,that the delay chain along with downsamplers form a serial-to-parallel(S/P) conversion. But as the number of branches is M and downsampling factor is only $M/2$ the filters $A_k(z^2)$ and $A_{k+M/2}(z^2)$ share a common delay line.

Applying the same logic to the synthesis filter the delay chain and upsamplers form a parallel-to-serial(P/S) converter with the output streams from polyphase filters $A_k(z^2)$ and $A_{k+M/2}(z^2)$ overlap with a delay.

For the analysis filter to be compatible with the OFDM ,it should be based on DFT. The figure below shows the DFT-based Analysis filter bank.

To obtain the DFT equivalent we flip the data stream entering the IDFT block upside down and multipliers have to be changed in a way such that both the implementations provide the same subchannel signals.

Let the input samples to the IDFT block be x_k and AFB output samples be z_k whereas the corresponding AFB output samples for DFT block be \tilde{z}_k .So the output samples can be written as

$$z_k = \left(\sum_{n=0}^{M-1} \exp(j \frac{2\pi kn}{M}) \cdot x_n \right) \beta_k \quad (1.12)$$

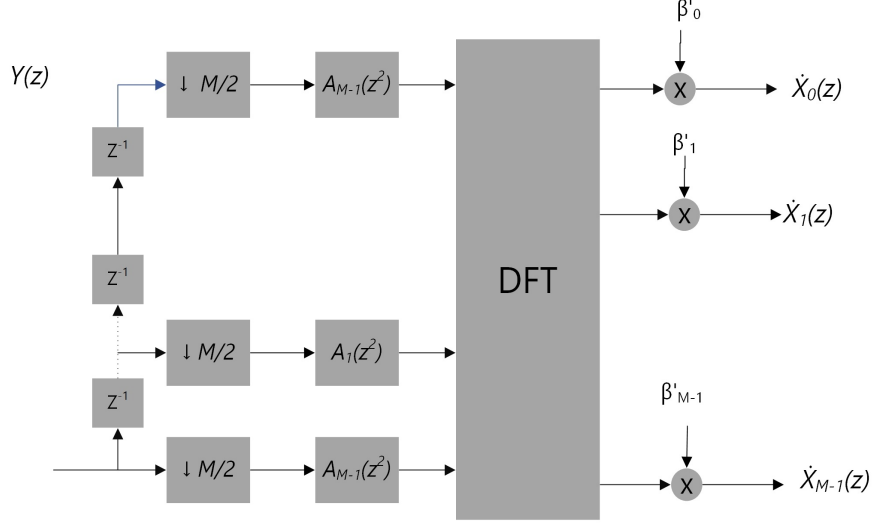


Figure 1.9: Analysis filter bank-DFT mode

and

$$\begin{aligned}\tilde{z}_k &= \left(\sum_{n=0}^{M-1} \exp(-j \frac{2\pi k n}{M}) x_{M-1-n} \right) \beta'_k \\ &= \left(\sum_{n=0}^{M-1} \exp(-j \frac{2\pi k (M-1-n)}{M}) x_n \right) \beta'_k\end{aligned}$$

So for $\tilde{z}_k = z_k$,

$$\begin{aligned}\beta'_k &= \exp(j \frac{2\pi k n}{M}) \exp(j \frac{2\pi k (M-1-n)}{M}) \beta_k \\ &= \exp(-j \frac{2\pi k}{M}) \beta_k \\ &= \exp(-j \frac{2\pi k}{M} (\frac{L_p + 1}{2}))\end{aligned} \tag{1.13}$$

Refer to Ari Viholainen (2010) for more details on polyphase implementation.

1.5 BER for FBMC under AWGN channel

1.5.1 BER for OFDM

The gaussian noise is defined by $\eta \sim \mathcal{N}(0, N_0)$. Let the transmitted symbols be $X[k]$. Then the received symbols are given by

$$\begin{aligned}\hat{x}[n] &= \mathcal{F}^{-1}(X[k]) + \eta[n]. \\ \mathcal{F}(\hat{x}[n]) &= X[k] + \mathcal{F}(\eta[n]). \\ \hat{X}[k] &= X[k] + \mathcal{F}(\eta[n])\end{aligned}\tag{1.14}$$

From the above equation we know that the signal corrupting QAM symbol $X[i]$ is $\mathcal{F}(\eta[n])$. Therefore for calculating BER we need to calculate its power i.e

$$\begin{aligned}E[\mathcal{F}(\eta[n])^2] &= E\left[\left(\frac{1}{\sqrt{N}} \sum_{m=0}^{N-1} \eta[n] e^{-j\frac{2\pi}{N}mk}\right)^2\right] \\ &= \frac{1}{N} \sum_{m=0}^{N-1} E[\eta^2[n]] e^{-j\frac{4\pi}{N}mk} = N_0\end{aligned}\tag{1.15}$$

1.5.2 BER for FBMC

Fig 1.7 and 1.9 combined represent FBMC structure. It is similar to OFDM except for the polyphase filters. OQAM can be seen as a special case of QAM which separates it into two symbols. We have seen that the delay chain and upsamplers are equivalent to P/S chain with OQAM symbols $M/2$ carriers apart overlapping i.e for a 16-OQAM though it appears to have two bits per OQAM sample, the overlap of two bits from the other carrier ensures 4 bits of information per sample of output to which the gaussian noise is added. From Eq 1.3 it is clear that filtering of the signal through polyphase filters doesn't alter the signal energy.

Therefore as signal energy and number of bits per sample of output added with noise are the same we have same energy per bit E_b in OFDM and FBMC. This implies (Refer Qinwei He (2015) for more detailed description) that the BER expression for an M -ary rectangular QAM or OQAM is same under AWGN channel for OFDM and FBMC i.e.,

$$BER \approx \frac{\sqrt{M} - 1}{\sqrt{M} \log_2 \sqrt{M}} Q \left[\sqrt{\frac{3 \log_2 M}{2(M-1)}} \cdot \frac{E_b}{N_0} \right], \quad (1.16)$$

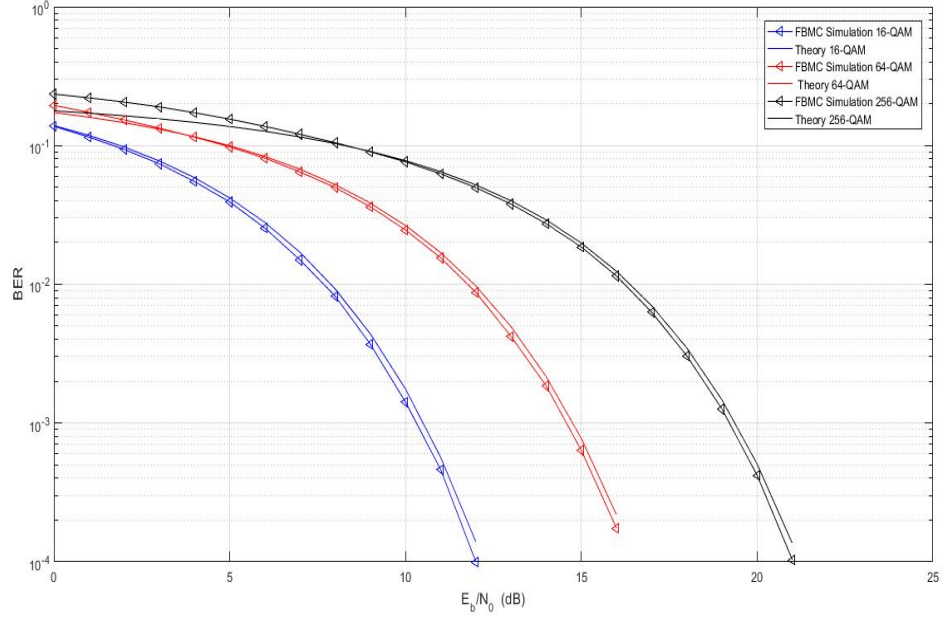


Figure 1.10: Bit Error Rate vs E_b/N_0 for FBMC simulation under AWGN

The theoretical ber given in Eq. 1.16 is obtained after neglecting the probability of error higher than that which demodulates it to it's adjacent symbol.

In the figure observe that the Bit Error rate for simulated 256 QAM is higher than that calculated theoritically at low $\frac{E_b}{N_0}$. This is due to the fact that at high noise variance and higher modulation, the error due to non adjacent symbol shifts is not negligible.

CHAPTER 2

MMSE Per-subchannel Equalizer

2.1 Introduction

The overview of the FBMC system with equaliser is shown in Fig 2.1. When vectors are denoted by $x[n]$, they represent $(N+1)$ dimensional vector $[x[n], x[n-1], \dots, x[n-N]]^T$ where N is given. I_N denotes $N \times N$ identity matrix and e_v represents unit vector with one at v^{th} position.

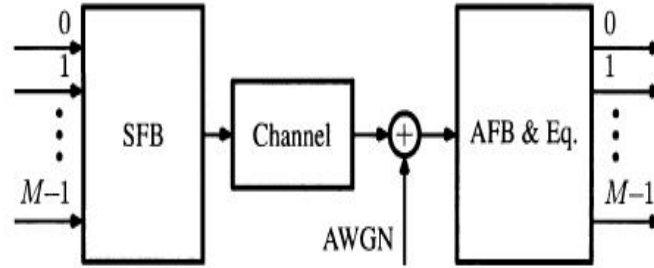


Figure 2.1: FBMC system overview

Fig. 2.2 shows the sub carrier model of FBMC and with it, the important aspect of the equaliser design i.e an equaliser is used per every subchannel. The FIR equaliser is used to compensate for both ISI and ICI in the given sub channel caused by the frequency selective channel response. The equaliser is $T/2$ spaced which allows it to remove ICI from the adjacent channels.

Fig. 2.3 shows the desired OQAM impulse response. The information in the real part of the equalised output is not influenced by the imaginary part and so the equaliser need not force it to zero. The stems with x marks are allowed to contain arbitrary values but the ones with filled circles have to be zero to avoid ISI on downsampling by 2.

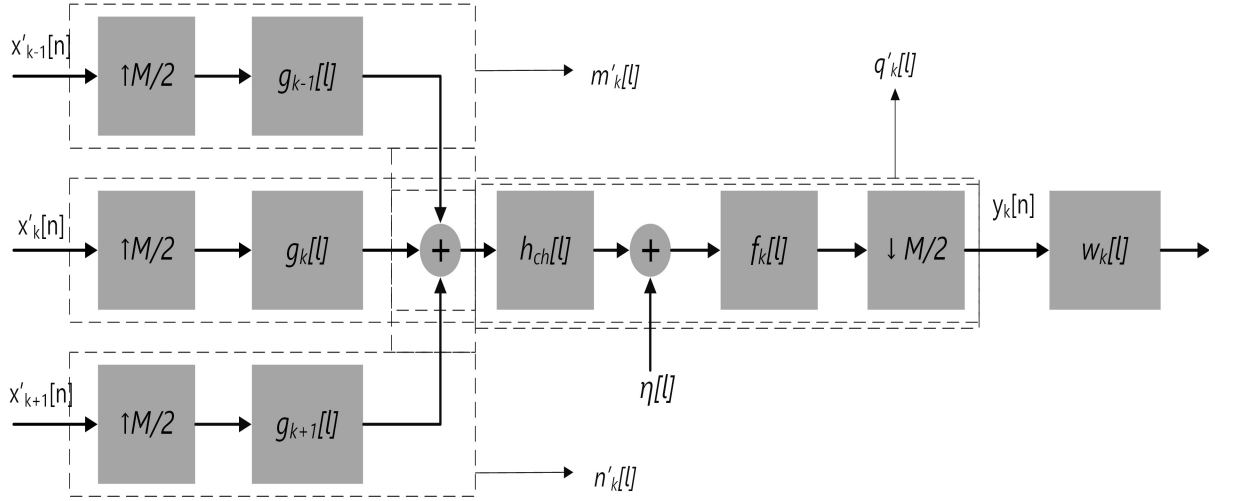


Figure 2.2: Sub carrier model for FBMC

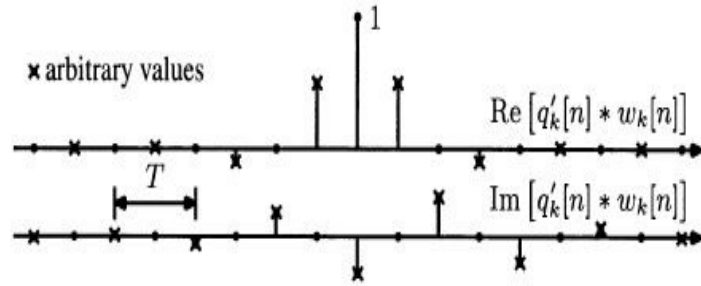


Figure 2.3: Desired OQAM impulse response

Since the subcarrier signals are orthogonally multiplexed we need to modify the conventional MMSE by dividing it into parts which operate on real and imaginary parts of the input seperately.

2.2 Derivation of MMSE Equalizer co-efficients

We will express input to the equaliser taking into account the interference from the adjacent sub channels and channel with the noise. The desired output response is set by considering the synthesis-analysis cascade of the given sub channel filter. Therefore on equalisation we get signal which is free of interference and channel distortion.

From Fig. 2.2 the received signal on sub channel filter $y_k[n] \in \mathcal{C}^N$ is given by,

$$y_k[n] = Q'_k x'_k[n] + M'_k x'_{k-1}[n] + N'_k x'_{k+1}[n] + \Gamma_k \eta[l] \quad (2.1)$$

where $x'_k[n] \in \mathcal{C}^L$

and $Q'_k, M'_k, N'_k \in \mathcal{C}^{N \times L}$ are the convolution matrices of the impulse responses $q'_k[n], m'_k[n], n'_k[n] \in \mathcal{C}^Q$ shown in Fig. 2.2 and Γ_k is the convolution matrix of analysis filter downsampled by $M/2$. Here $L = N + Q - 1$ which is number of columns of convolution matrix is dictated by the length Q of filter impulse responses. The output of the analysis filter is then sent through the equaliser. The real and imaginary part of OQAM output are then obtained in the same order as input sent through the carrier by OQAM post processing as shown in Fig. 1.3 i.e.,

$$\begin{aligned} \tilde{a}_k[m] &= \text{Re}(w_k^H y_k[n]) \\ &= \begin{bmatrix} w_k^{(R),T} & w_k^{(I),T} \end{bmatrix} \begin{bmatrix} y_k^{(R)}[n] \\ y_k^{(I)}[n] \end{bmatrix} \\ \tilde{b}_k[m] &= \text{Im}(w_k^H y_k[n-1]) \\ &= \begin{bmatrix} -w_k^{(I),T} & w_k^{(R),T} \end{bmatrix} \begin{bmatrix} y_k^{(R)}[n-1] \\ y_k^{(I)}[n-1] \end{bmatrix} \quad \text{where } n = 2m \\ \text{and } \tilde{a}_k[m] &= \text{Re}(w_k^H y_k[n-1]) \\ \tilde{b}_k[m] &= \text{Im}(w_k^H y_k[n]) \quad \text{where } n = 2m + 1 \end{aligned} \quad (2.2)$$

and the output data symbol is $\tilde{c}_k[m] = \tilde{a}_k[m] + j\tilde{b}_k[m]$. The estimated data symbol $\hat{c}_k[n]$ is obtained by taking a hard decision on $\tilde{c}_k[n]$

We intend to minimise $E[|\hat{a}_k[m] - a_k[m - \nu]|^2]$ or $E[|\hat{b}_k[m] - b_k[m - \nu]|^2]$.

From H.syed (2008) we see that the optimal MMSE equalizer coefficients are given by

Wiener-Hopf equation

$$R_{yy}w_{opt} = p \quad (2.3)$$

Here $R_{yy} = E[yy^H]$ denotes the auto-correlation of the input $y[n]$ to the equaliser whereas $p = E[\hat{y}.y^H]$ is the cross correlation between the desired output $\hat{y}[n]$ and the input of the equaliser.

As discussed previously we need to modify the MMSE into real and imaginary parts to process the OQAM inputs seperately i.e.,

$$\begin{aligned} y_k^{(R)}[n] &\approx Q_k^{(R)}x_k[n] + M_k^{(R)}x_{k-1}[n] + N_k^{(R)}x_{k+1}[n] + Re[\Gamma_k\eta[l]] \\ y_k^{(I)}[n] &\approx Q_k^{(I)}x_k[n] + M_k^{(I)}x_{k-1}[n] + N_k^{(I)}x_{k+1}[n] + Im[\Gamma_k\eta[l]] \end{aligned} \quad (2.4)$$

The above equations are obtained by applying real and imaginary part to Eq2.1 after shifting j of each imaginary entry of $x'_k[n]$ and multiplying the alternate columns of Q'_k with it,giving Q_k .Same applies for N_k, M_k Combining both the equations in Eq. 2.4 and writing them compactly

$$Y_k = \begin{bmatrix} y_k^R \\ y_k^I \end{bmatrix} = H_k x_k[n] + F_k \begin{bmatrix} x_{k-1}[n] \\ x_{k+1}[n] \end{bmatrix} + \begin{bmatrix} Re(\Gamma_k\eta[l]) \\ Im(\Gamma_k\eta[l]) \end{bmatrix} \quad (2.5)$$

where $H_k = \begin{bmatrix} Q_k^{(R)} \\ Q_k^{(I)} \end{bmatrix}$ and $F_k = \begin{bmatrix} M_k^{(R)} & N_k^{(R)} \\ M_k^{(I)} & N_k^{(I)} \end{bmatrix}$

Now we have to apply Wiener-Hopf equation taking $y_k[n]$ as input and $x_k[n - \nu]$ as the desired output where the delay ν depends on filters ,channel response and is equal to $((L_p - 1) + length(h_{ch})/2)/(M/2)$.So we have

$$R_{yy} = E[Y_k Y_k^H] \quad \text{and} \quad R_{yx} = E[Y_k x_k^H(n - \nu)] \quad (2.6)$$

Assuming that signal inputs to different sub carriers are uncorrelated and all the sub channel signals possess the same statistics.We have :

$$\begin{aligned} E[x_p[n]x_q^H[n]] &= 0 \quad \text{when } p \neq q \\ &= \frac{\sigma_d^2}{2} I_L \quad \text{when } p = q \end{aligned} \quad (2.7)$$

Applying Eqs. 2.5,. 2.6,. 2.7 in . 2.1 we get

$$w'_{k,MMSE} = [H_k R_x H_k^T + F_k \hat{R}_x F_k^T + R_{\eta,k}]^{-1} H_k R_x e_\nu \quad (2.8)$$

where $\hat{R}_x = \begin{bmatrix} R_x & 0 \\ 0 & R_x \end{bmatrix}$; $R_{\eta,k} = \frac{\sigma_\eta^2}{2} \Gamma'_k \Gamma'^T_k$; $\Gamma'_k = \begin{bmatrix} \Gamma_k^{(R)} & \Gamma_k^{(I)} \\ -\Gamma_k^{(I)} & \Gamma_k^{(R)} \end{bmatrix}$

Further simplifying Eq. 2.8 by substituting R_{xx} from Eq. 2.7 gives

$$w'_{k,MMSE} = [H_k H_k^T + F_k F_k^T + R_{\eta,k}]^{-1} H_k e_\nu \quad (2.9)$$

Since we have derived equaliser coefficients $w'_{k,MMSE}$ by seperating real and imaginary parts,we have

$$w_k'^T = [w_k^{(R),T}, w_k^{(I),T}] \in \mathcal{R}^{2N}$$

2.3 Simulation of MMSE Equalisation

In this simulation the proposed per-sub carrier equaliser will be simulated for a Vehicular A channel which is 50 taps long.The cyclic prefix in OFDM takes out any ISI that may be present.But FBMC has to equalise to remove the interference.For both the system we use a bandwidth of $10MHz$ and $f_s = 15.36MHz$.In FBMC we use $M = 1024, 512, 256$ carriers in which data is transmitted. The OFDM on the other hand has $N_{cp} = 256, M_0 = 1024$ giving 80 percent redundancy.To ensure the same bandwidth efficiency i.e bits/s/Hz the performance of 32-QAM OFDM is compared with 16-QAM FBMC since OFDM symbol is 5M/4 long and 5/4 times the bits results in the same efficiency.

We compare the number of equaliser taps needed to compensate for increase in the frequency selectivity and the increase in complexity for FBMC. BER for 16-QAM OFDM is considered as reference for perfect equalisation though it gives only 80 percent of throughput when compared to others.

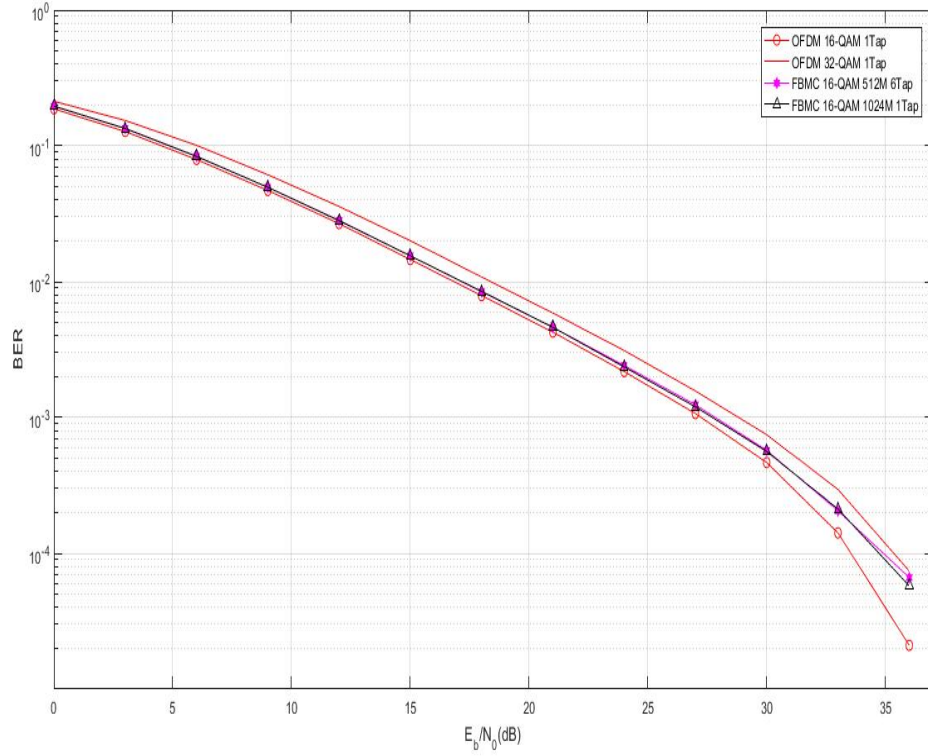


Figure 2.4: Comparison of FBMC with CP-OFDM

Comparison of complexity : We compare the complexity of FBMC equalisation by the number of real multiplications that occur within one OFDM symbol ($M_0 t_s$).

OFDM : $2N_{fft}(M_0)$ multiplications for FFT/IFFT operations

$4M_0$ multiplications for 1-Tap equalisation.

FBMC : M_0/M FBMC symbols are processed for a single OFDM symbol.

Per One FBMC symbol-

$4N_{fft}(M)$ for FFT/IFFT as they are processed at twice the sample rate

$8(KM + 1)$ multiplications for polyphase filtering

$4MN$ multiplications for N-tap equalisation.

$$\text{Ratio of complexity}(\gamma) = \frac{N_{FBMC}}{N_{OFDM}} = \frac{M_0}{M} \frac{4N_{fft}(M) + 8(KM + 1) + 4MN}{2N_{fft}(M_0) + 4M_0}$$

where $N_{fft}(M) = M(\log_2(M) - 3) + 4$ multiplications using split radix algorithm for M-FFT/IFFT.

Conclusion : It can be seen that 1, 6 taps give similar performance in BER to CP-OFDM with $\gamma = 2, 2.5$ for $M = 1024, 512$ respectively. The FBMC requires a more powerful equaliser in terms of taps and therefore computation when M is decreased due to the increased frequency selectivity in sub channel. We have more flexibility in choosing number of sub-carriers in FBMC unlike OFDM where M is set to higher value to decrease the redundancy in the system. FBMC leads to lesser out-of band emissions and the flexibility in choosing lesser M which decreases the sensitivity against carrier frequency offset. Refer Dirk S. Waldhauser and A. Nossek (2008) for more details.

For $M = 256$ with the same channel as above, BER is shown in Fig. 2.5. It can be

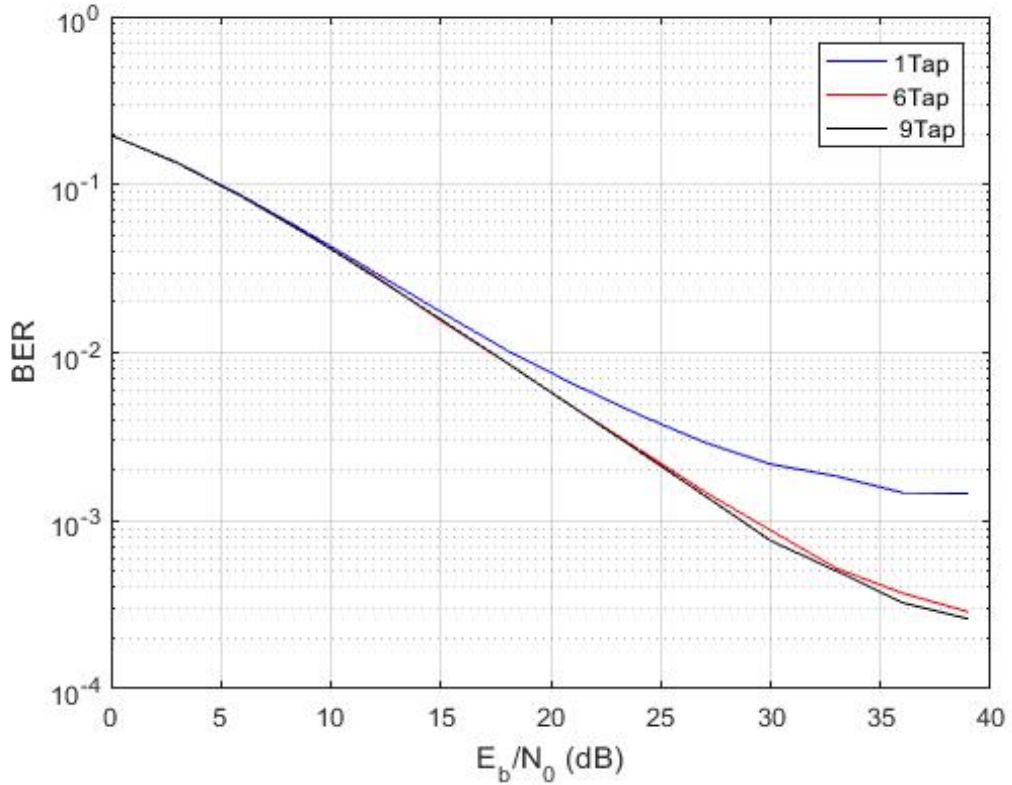


Figure 2.5: Comparison of MMSE Equalisation with $M=256$ and different taps

seen that the Bit-error-rate is flooring after a certain $\frac{E_b}{N_0}$. It can be said that the equaliser is not effectively removing the interference from adjacent sub-carriers. In the next section we use a Two stage MMSE equalizer which deals with ICI and ISI in two stages separately.

2.4 Two-stage MMSE

We can see that per subchannel MMSE takes into account the interference from adjacent subchannels. But from Fig. 2.5 we see that the BER floors after certain E_b/N_0 which implies that there is still interference left. Therefore we employ two stages to equalise so that interference is removed effectively. We first apply the MMSE equalisation to recover the transmitted symbols.

Assuming these intermediate symbols are correctly decoded, we then use these symbols from the adjacent sub-carriers to subtract the inter carrier interference. These intermediate decisions are not used to eliminate interference in the same subcarrier so as to limit the order of error propagation that might occur. Then another MMSE equaliser void of the interference terms of Eq. 2.9 can be derived to suppress Inter-symbol interference. The process can be described briefly in the following two steps.

Step 1: As described above, MMSE equalisation is applied to remove ICI. Let $\tilde{x}_k[n]$ be the equalised output, which undergoes OQAM post processing as shown in Fig. 1.3 to give $\tilde{c}_k[m]$ and $\hat{c}_k[m]$ be obtained by taking a hard decision on $\tilde{c}_k[m]$.

Assuming this is correct i.e $\hat{c}_k[m] = c_k[m]$ for most part, we obtain the vector $\hat{x}'_k[n]$ by remodulating $\hat{c}_k[m]$ i.e OQAM modulating $\hat{c}_k[m]$ considering it as input. Now consider Eq. 2.5 after obtaining $\hat{x}_k[n]$ from $\hat{x}'_k[n]$ by shifting j of each imaginary entry into G_k . We then calculate the interference term in the RHS of the equation after estimating the channel and calculating F_k . Therefore from Eq. 2.5

$$Y_k^- = Y_k - F_k \begin{bmatrix} \hat{x}_{k-1}[n] \\ \hat{x}_{k+1}[n] \end{bmatrix} \approx H_k x_k[n] + \begin{bmatrix} Re(\Gamma_k \eta[l]) \\ Im(\Gamma_k \eta[l]) \end{bmatrix} \quad (2.10)$$

as we assumed $\hat{c}_k[m] = c_k[m]$ which implies $\hat{x}_k[n] = x_k[n]$

Step 2: It can be seen from Eq. 2.10 that the signal is rid of ICI. Applying the same series of steps from Eq. 2.5 to Eq. 2.9 on Eq 2.10 we get

$$w'_{k,MMSE} = [H_k H_k^T + R_{\eta,k}]^{-1} H_k e_\nu \quad (2.11)$$

This equaliser takes care of ISI in the sub-carrier signal. We increase the complexity of equaliser to gain BER performance. Since the terms in the second stage are same as

the original, they can be calculated alongside. Refer Ikhlef and Louveax (2009) for more details.

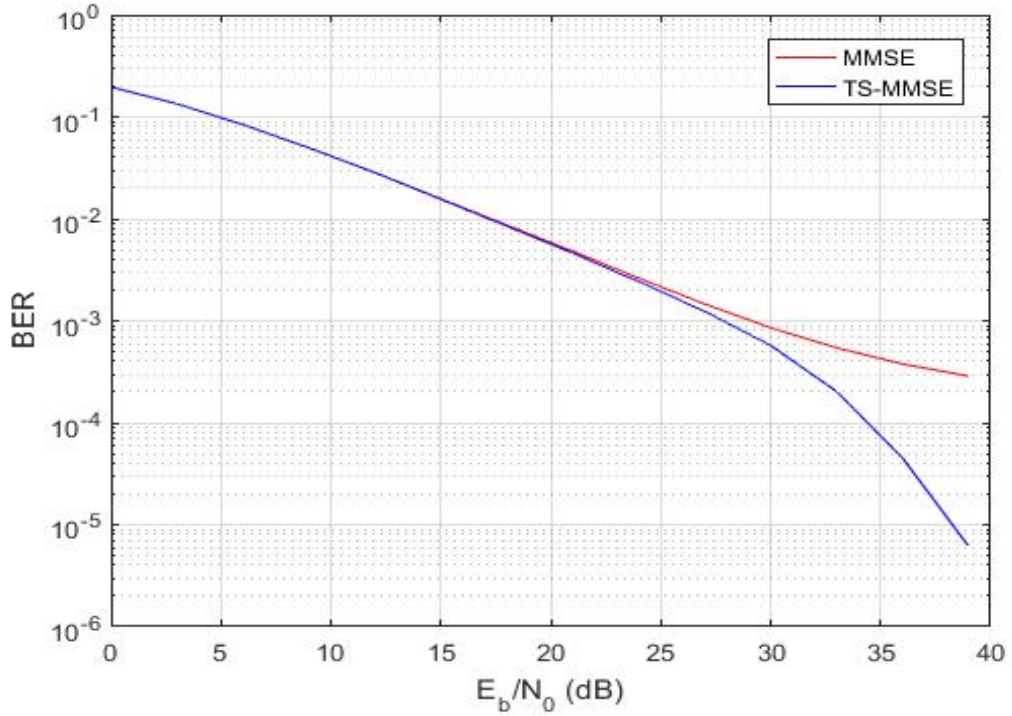


Figure 2.6: Two stage MMSE Equalisation with $M=256$ and 6 taps

Conclusion :

From the flooring of BER you can see that the equaliser given by Eq. 2.9 couldn't effectively get rid of the interference. The term of the equaliser equation which tries to remove the interference is $F_k F_k^T$.

The interference in a given sub channel very much depends on the data in adjacent sub-channels, but the equaliser being sub-channel wise takes in the data only from that sub carrier and relies on assumptions of zero cross correlation between data of adjacent carriers to remove interference. Whereas TS-MMSE uses that equalised data after making hard decision on symbols to approximate the interference in the sub carriers. After removing the interference from the input to the original equaliser, the output data is sent through equaliser of Eq. 2.11 to remove ISI from symbols in the same sub-carrier.

CHAPTER 3

Channel estimation

3.1 Channel model

In this section we consider the baseband equivalent of signals. The transmitted FBMC signal is filtered by channel impulse response $h_{ch}(t, \tau)$ and additive white gaussian noise $\eta(t)$ is added.

$$r(t) = (h_{ch} * s)(t) + \eta(t) \quad (3.1)$$

Let $(x_k[n])_{\uparrow M/2} = x_k''[n]$ and

$$\begin{aligned} s(t) &= \sum_{k=0}^{M-1} \sum_{n \in \mathbb{Z}} x_k''[n] g_{k,n}(t) \\ &= \sum_{k=0}^{M-1} \sum_{n \in \mathbb{Z}} x_k''[n] p(t - nt_0/2) e^{j2\pi k f_0 t} \theta_{k,n} \beta_k \end{aligned} \quad (3.2)$$

Here $x_k''[n]$ are real-valued, $p(t)$ is the synthesis prototype filter. $f_0 = 1/t_0$ where t_0 is the symbol period.

Let τ_0 be the maximum delay spread in the channel. Then from Eqs. 3.1 and 3.2 we get

$$\begin{aligned} r(t) &= \sum_{n=-\infty}^{\infty} \sum_{k=0}^{M-1} x_k''[n] \int_0^{\tau_0} h_{ch}(t, \tau) g_{k,n}(t - \tau) d\tau + \eta(t) \\ &= \sum_{n=-\infty}^{\infty} \sum_{k=0}^{M-1} x_k''[n] \theta_{k,n} \beta_k e^{j2\pi k f_0 t} \times \int_0^{\tau_0} h_{ch}(t, \tau) p(t - \tau - nt_0/2) e^{-j2\pi k f_0 \tau} d\tau + \eta(t) \end{aligned} \quad (3.3)$$

Assuming we have a flat-fading channel at each sub-carrier i.e the coherence bandwidth of the channel $\frac{1}{2\tau_0} > \frac{1}{L_p}$ where $L_p = Kt_0$ is the length of prototype filter. Then prototype filter is almost constant in the interval $[0, \tau_0]$ in the integral in Equation above, therefore

$$r(t) = \sum_{n=-\infty}^{\infty} \sum_{k=0}^{M-1} x_k''[n] g_{k,n}(t) H_k(t) + \eta(t) \quad (3.4)$$

where

$$H_k(t) = \int_0^{\tau_0} h_{ch}(t, \tau) e^{-j2\pi k f_0 \tau} d\tau$$

i.e $H_k(t)$ is the frequency response of the channel at instant t .

Assuming channel response remains constant during the duration of the prototype filter, we have $H_k(t) = H_k[n]$. Putting this in Eq. 3.4 we get :

$$\begin{aligned} r(t) &= \sum_{n=-\infty}^{\infty} \sum_{k=0}^{M-1} x_k''[n] g_{k,n}(t) H_k[n] + \eta(t) \\ \text{i.e } r[l] &= \sum_{n=-\infty}^{\infty} \sum_{k=0}^{M-1} x_k''[n] g_{k,n}[l] H_k[n] + \eta[l] \end{aligned} \quad (3.5)$$

$$\text{where } g_{k,n}[l] = p[l - nM/2] e^{j\frac{2\pi}{M} ml} \theta_{k,n}$$

$f_{k,n}[l] = p[l - nM/2] e^{j2\pi k f_0 l} \beta_k \theta_{k,n}^*$. Now ignoring the noise, the received symbol $y_{k_0}[n_0]$ is given by :

$$\begin{aligned} y_{k_0}[n_0] &= x_{k_0}[n_0] \langle g * f \rangle_{k_0, n_0}^{k_0, n_0} H_{k_0}[n_0] \\ &+ \sum_{(k,n) \neq (k_0, n_0)} x_k[n] H_k[n] \langle g * f \rangle_{k_0, n_0}^{k, n} + (\eta[n] * f_{k,n}[l])_{\downarrow M/2} \end{aligned} \quad (3.6)$$

$$\text{where } \langle g * f \rangle_{k_0, n_0}^{k, n} = (g_{k_0, n_0}[l] * f_{k,n}[l]) \text{ at } nM/2$$

In absence of channel i.e $H_k[n] = 1$ and $\eta = 0$ you can see that $\langle g * f \rangle$ is the impulse response of the system with respect to $x_k[n]$. Table.(1.1) refers to the impulse response of the transmitter receiver cascade and is the impulse response with respect to $x_k'[n]$. It includes both β_k and $g(t - nt_0/2)$. We have to multiply the table by $\theta_{k,n}$ to get the impulse response w.r.t $x_k[n]$ i.e multiply the 1 in the centre with 1 and alternately with j in the same row. Multiply the element above 1 with j and alternately multiply with 1 and j . Then we get :

↓subch,time→	n-4	n-3	n-2	n-1	n	n+1	n+2	n+3	n+4
k-1	j0.005	j 0.043	-j0.125	-j0.206	j0.239	j 0.206	-j0.125	-j0.043	j0.005
k	0	-j0.067	0	j0.564	1	j0.564	0	-j0.067	0
k+1	j0.005	j 0.043	-j0.125	-j0.206	j0.239	j 0.206	-j0.125	-j0.043	j0.005

Table 3.1: Impulse response of the filter bank transmission system w.r.t $x_{k,n}$ at $\mathbf{K} = 4$

From the table it is clear that $\mathcal{R}\{\langle g * f \rangle_{k_0, n_0}^{k, n}\} = 0$ unless $k = k_0$ and $n = n_0$. Therefore the summation term in R.H.S of the Eq. 3.6 is purely imaginary in absence of channel. Therefore 1 tap ZF equalised signal can be written as

$$\frac{y_{m_0}[n_0]}{H_{m_0}[n_0]} = x_{k_0}[n_0] + I_{k_0, n_0}$$

where $I_{k_0, n_0} = \sum_{(k, n) \neq (k_0, n_0)} x_k[n] \frac{H_k[n]}{H_{k_0}[n_0]} \langle g * f \rangle_{k_0, n_0}^{k, n}$

Then the estimated symbol is given by:

$$\begin{aligned} \hat{x}_{k_0}[n_0] &= \mathcal{R}\left\{ \frac{y_{k_0}[n_0]}{H_{k_0}[n_0]} \right\} \\ &= x_{k_0}[n_0] + \mathcal{R}\{I_{k_0, n_0}\}. \end{aligned}$$

Here $\mathcal{R}\{I_{m_0, n_0}\}$ represents ISI between the real symbols. We can't get an accurate estimate of $x_{m_0}[n_0]$ due to ISI. Let's say there exists $(\delta k, \delta n)$ both positive such that $H_k[n] \approx H_{k_0}[n_0]$ whenever $|k - k_0| < \delta k, |n - n_0| < \delta n$. This values of $\delta k, \delta n$ depends on the coherence bandwidth $\frac{1}{2\delta}$. When it decreases so does δk and the same relation is valid for coherence time and δn . Generally coherence bandwidth occupies more than few sub carriers i.e channel response is same for $\delta_k > 1$. Also coherence time is greater than t_0 i.e $\delta n > 1$. Then we can write

$$\begin{aligned} \frac{y_{k_0}[n_0]}{H_{k_0}[n_0]} &= x_{k_0}[n_0] \\ &+ \sum_{\substack{|k-k_0| < \delta k, |n-n_0| < \delta n \\ (k, n) \neq (k_0, n_0)}} x_k[n] \langle g * f \rangle_{k_0, n_0}^{k, n} \\ &+ \sum_{|k-k_0| > \delta k, |n-n_0| > \delta n} x_k[n] \frac{H_k[n]}{H_{k_0}[n_0]} \langle g * f \rangle_{k_0, n_0}^{k, n} \end{aligned}$$

From the table above you can see that $\langle g * f \rangle_{k_0, n_0}^{k, n}$ decays rapidly as one moves beyond the very successive neighborhood of the centre i.e., when $(|k - k_0|, |n - n_0|) < (1, 1) < (\delta k, \delta n)$. This is because the filter is well localised in time and frequency. Therefore in equation for I_{k_0, n_0} we can ignore the terms for which $(|k - k_0|, |n - n_0|) > (\delta k, \delta n)$

which gives :

$$\begin{aligned} \frac{y_{k_0}[n_0]}{H_{k_0}[n_0]} &= x_{k_0}[n_0] \\ &+ \sum_{\substack{|k-k_0| < \delta k, |n-n_0| < \delta n \\ (k,n) \neq (k_0,n_0)}} x_k[n] \langle g * f \rangle_{k_0,n_0}^{k,n} \end{aligned} \quad (3.7)$$

Let $x_{k_0}^{(i)}[n_0]$ denote the imaginary part of interference of other symbols on $x_{k_0}[n_0]$.Then

$$x_{k_0}^{(i)}[n_0] = -j \sum_{\substack{|k-k_0| < \delta k, |n-n_0| < \delta n \\ (k,n) \neq (k_0,n_0)}} x_k[n] \langle g * f \rangle_{k_0,n_0}^{k,n} \quad (3.8)$$

Then from two equations above we have $y_{k_0}[n_0] \approx H_{k_0}[n_0](x_{k_0}[n_0] + jx_{k_0}^{(i)}[n_0])$

3.2 Interference Approximation method(IAM)

The preamble is assumed to be perfectly known to the receiver. We have a redundancy of atleast $3t_0/2$ when it comes to OQAM modulation i.e., we lose $3M$ real data or $3M/2$ complex data. As discussed in the previous section after applying some approximations over the locality of channel response and the filter response ,we can express the interference on any symbol in terms of adjacent symbols i.e imaginary terms can be approximated as :

$$x_{k_0}^{(i)}[n_0] \approx \sum_{|k-k_0|=1, |n-n_0|=1} x_k[n] \langle g * f \rangle_{k_0,n_0}^{k,n} \quad (3.9)$$

In absence of noise ,the channel can be estimated as :

$$H_{wn,k_0}[n_0] = \frac{y_{k_0}[n_0]}{x_{k_0}[n_0] + jx_{k_0}^{(i)}[n_0]} \quad (3.10)$$

In presence of noise η the estimated channel is :

$$H_{k_0}[n_0] = H_{wn,k_0}[n_0] + \frac{\eta}{x_{k_0}[n_0] + jx_{k_0}^{(i)}[n_0]} \quad (3.11)$$

As you can see the error in estimation comes from the second term and can be minimised by increasing it's power. First let's look at the general case of preamble ,i.e the

real symbols are chosen at random but have a variance of σ_x^2 . Consider the power of $z_{k_0}[n_0] = x_{k_0}[n_0] + jx_{k_0}^{(i)}[n_0]$, we have :

$$\begin{aligned} E(z_{k_0}[n_0]) &= 0 \\ E(|z_{k_0}[n_0]|^2) &= \sigma_x^2 \left(1 + \sum_{\substack{|k-k_0| < \delta k, |n-n_0| < \delta n \\ (k,n) \neq (k_0,n_0)}} |\langle g * f \rangle_{k_0,n_0}^{k,n}|^2 \right) \end{aligned} \quad (3.12)$$

In C.Lele and P.Siohan (2007) it is proved that:

$$\sum_{(k,n) \neq (k_0,n_0)} \left| \langle g * f \rangle_{k_0,n_0}^{k,n} \right|^2 = 1 \quad (3.13)$$

As we already know that the filter is concentrated in the immediate neighbourhood we have $E(|z_{k_0}[n_0]|) \approx 2\sigma_x^2$

To increase the power we can choose the preamble in such a way that all the terms in the interference have the same sign ,then

$$\begin{aligned} E(|z_{k_0}[n_0]|^2) &= \sigma_x^2 \left(\sum_{\substack{|k-k_0| < \delta k, |n-n_0| < \delta n \\ (k,n) \neq (k_0,n_0)}} |\langle g * f \rangle_{k_0,n_0}^{k,n}| \right)^2 \\ &\geq \sigma_x^2 \sum_{\substack{|k-k_0| < \delta k, |n-n_0| < \delta n \\ (k,n) \neq (k_0,n_0)}} (|\langle g * f \rangle_{k_0,n_0}^{k,n}|^2) \\ &\geq \sigma_x^2 \end{aligned} \quad (3.14)$$

Therefore we can increase the power of $z_{k_0}[n_0]$ and thus improve the performance. We can have multiple combinations of preambles adding up the interference term. One of the possible preambles doing that is used in the simulation.

3.3 Pair of Pilots scheme (POP)

This method is based on insertion of pair of pilots (POP) at positions known by the receiver. The pilots are preferably placed in the consecutive time positions with same sub-carrier index so that the assumption that channel response is invariant is satisfied. Let

$(k_1, n_1), (k_2, n_2)$ be the reference symbol positions. Then we have :

$$\begin{aligned} y_{k_1}[n_1] &= H_{k_1}[n_1](x_{k_1}[n_1] + jx_{k_1}^{(i)}[n_1]) \\ y_{k_2}[n_2] &= H_{k_2}[n_2](x_{k_2}[n_2] + jx_{k_2}^{(i)}[n_2]) \end{aligned} \quad (3.15)$$

Let C be the ratio between the real and imaginary parts of H_{k_1, n_1} i.e $H_{k_1}[n_1] = H_{k_1}^{(r)}[n_1] + jH_{k_1}^{(i)}[n_1]$ and $C = H_{k_1}^{(i)}[n_1]/H_{k_1}^{(r)}[n_1]$. Taking real and imaginary parts of Eq() we get :

$$\begin{aligned} y_{k_1}^{(r)}[n_1] &= H_{k_1}^{(r)}[n_1]x_{k_1}[n_1] - CH_{k_1}^{(r)}[n_1]x_{k_1}^{(i)}[n_1] \\ y_{k_1}^{(i)}[n_1] &= CH_{k_1}^{(r)}[n_1]x_{k_1}[n_1] + H_{k_1}^{(r)}[n_1]x_{k_1}^{(i)}[n_1] \\ y_{k_2}^{(r)}[n_2] &= H_{k_2}^{(r)}[n_2]x_{k_2}[n_2] - CH_{k_2}^{(r)}[n_2]x_{k_2}^{(i)}[n_2] \\ y_{k_2}^{(i)}[n_2] &= CH_{k_2}^{(r)}[n_2]x_{k_2}[n_2] + H_{k_2}^{(r)}[n_2]x_{k_2}^{(i)}[n_2] \end{aligned} \quad (3.16)$$

As we assumed channel is invariant we have $H_{k_1}[n_1] = H_{k_2}[n_2]$. Putting this in the above equation and by combination of above equations we get:

$$\begin{aligned} X_1 &= x_{k_2}[n_2]y_{k_1}^{(r)}[n_1] - x_{k_1}[n_1]y_{k_2}^{(r)}[n_2] \\ &= CH_{k_1}^{(r)}[n_1](-x_{k_2}[n_2]x_{k_1}^{(i)}[n_1] + x_{k_1}[n_1]x_{k_2}^{(i)}[n_2]) \\ X_2 &= x_{k_2}[n_2]y_{k_1}^{(i)}[n_1] - x_{k_1}[n_1]y_{k_2}^{(i)}[n_2] \\ &= H_{k_1}^{(r)}[n_1](x_{k_2}[n_2]x_{k_1}^{(i)}[n_1] - x_{k_1}[n_1]x_{k_2}^{(i)}[n_2]) \end{aligned} \quad (3.17)$$

Then the ratio X_1/X_2 gives :

$$C = \frac{x_{k_2}[n_2]y_{k_1}^{(r)}[n_1] - x_{k_1}[n_1]y_{k_2}^{(r)}[n_2]}{x_{k_1}[n_1]y_{k_2}^{(i)}[n_2] - x_{k_2}[n_2]y_{k_1}^{(i)}[n_1]} \quad (3.18)$$

Then the first two equations in Eq. 3.16 can be rewritten as :

$$\begin{aligned} y_{k_1}^{(r)}[n_1] &= H_{k_1}^{(r)}[n_1]x_{k_1}[n_1] - CH_{k_1}^{(r)}[n_1]x_{k_1}^{(i)}[n_1] \\ Cy_{k_1}^{(i)}[n_1] &= C^2H_{k_1}^{(r)}[n_1]x_{k_1}[n_1] + CH_{k_1}^{(r)}[n_1]x_{k_1}^{(i)}[n_1] \end{aligned}$$

Adding the above equations we get :

$$\begin{aligned}
H_{k_1}^{(r)}[n_1]x_{k_1}[n_1](1 + C^2) &= y_{k_1}^{(r)}[n_1] + Cy_{k_1}^{(i)}[n_1] \\
H_{k_1}^{(r)}[n_1] &= \frac{y_{k_1}^{(r)}[n_1] + Cy_{k_1}^{(i)}[n_1]}{x_{k_1}[n_1](1 + C^2)} \\
\text{and } H_{k_1}^{(i)}[n_1] &= CH_{k_1}^{(r)}[n_1]
\end{aligned} \tag{3.19}$$

POP doesn't require any knowledge of prototype filter and can be used by preamble based or scattered based channel estimation. In presence of noise the equations $X1, X2$ becomes

$$\begin{aligned}
Y_1 &= CH_{k_1}^{(r)}[n_1](-x_{k_2}[n_2]x_{k_1}^{(i)}[n_1] + x_{k_1}[n_1]x_{k_2}^{(i)}[n_2]) + \eta_1 \\
Y_2 &= H_{k_1}^{(r)}[n_1](x_{k_2}[n_2]x_{k_1}^{(i)}[n_1] - x_{k_1}[n_1]x_{k_2}^{(i)}[n_2]) + \eta_2
\end{aligned} \tag{3.20}$$

Therefore we have :

$$\begin{aligned}
\hat{C} &= \frac{Y_1}{Y_2} \\
&= C \frac{1 + \frac{\eta_1}{\nu H_{k_1}^{(i)}[n_1]}}{1 - \frac{\eta_2}{\nu H_{k_1}^{(i)}[n_1]}}
\end{aligned} \tag{3.21}$$

where : $\nu = -x_{k_2}[n_2]x_{k_1}^{(i)}[n_1] + x_{k_1}[n_1]x_{k_2}^{(i)}[n_2]$ The performance of the estimation depends on power of ν . If it's low then the noise term is magnified and the value of C is more distorted. As ν depends on $x_{k_1}^{(i)}[n_1], x_{k_2}^{(i)}[n_2]$ which are dependent on data other than those in the pilot positions. This leads to randomness which affects the performance of POP as you will see in the simulation below. Refer C. Lele and P. Siohan (2007) for a more detailed description of channel model and estimation methods.

3.4 Simulation results using channel estimation

We use the following preambles for Channel estimation :

0	1	0	$x_0[4]$	$x_0[5]$,	,	,
0	1	0	$x_1[4]$	$x_1[5]$,	,	,
0	1	0	$x_2[4]$	$x_2[5]$,	,	,
0	1	0	$x_3[4]$	$x_3[5]$,	,	,
,	,	,	,	,	,	,	,
,	,	,	,	,	,	,	,
,	,	,	,	,	,	,	,
,	,	,	,	,	,	,	,
0	1	0	,	,	,	,	,
0	1	0	$x_{M-1}[4]$	$x_{M-1}[5]$,	,	,

Table 3.2: OQAM/IAM

1	0	$x_0[3]$	$x_0[4]$	$x_0[5]$,	,	,
-1	0	$x_1[3]$	$x_1[4]$	$x_1[5]$,	,	,
1	0	$x_2[3]$	$x_2[4]$	$x_2[5]$,	,	,
-1	0	$x_3[3]$	$x_3[4]$	$x_3[5]$,	,	,
,	,	,	,	,	,	,	,
,	,	,	,	,	,	,	,
,	,	,	,	,	,	,	,
,	,	,	,	,	,	,	,
1	0	,	,	,	,	,	,
-1	0	$x_{M-1}[3]$	$x_{M-1}[4]$	$x_{M-1}[5]$,	,	,

Table 3.3: OQAM/POP

The same simulation parameters as in previous chapter are used. We consider $M = 256$ with no guard band and number of taps of equaliser $N = 6$. Vehicular channel of type A with 50 taps is used.

The choice of the preamble can be understood by taking a look at the table(3.1). In preamble of IAM the ones on the either side result in summing of interferences and thus increase the power of denominator in Eq. 3.11. Whereas in POP the sequence of ones in the first symbol results in summation of terms in $x_{k_2}^{(i)}[n_2]$ with n_2 being 2.

For PHYDYAS filter IAM, POP preambles that are shown above suffer from the same drawback. When higher modulations are used, say 16-QAM, the interference terms from two columns away from the centre of preamble lead to a significant distortion from the approximation we make. That is for example, $j0.125 * 3 > j0.2393 * 1$, interference

from second adjacent column is higher than the first, which we consider in the approximation and this affects the channel estimation. Therefore 4-QAM is used to mitigate this effect. A well localised filter in time or a larger preamble of $5t_0/2$ in IAM can be used to better the approximation retaining 16-QAM.

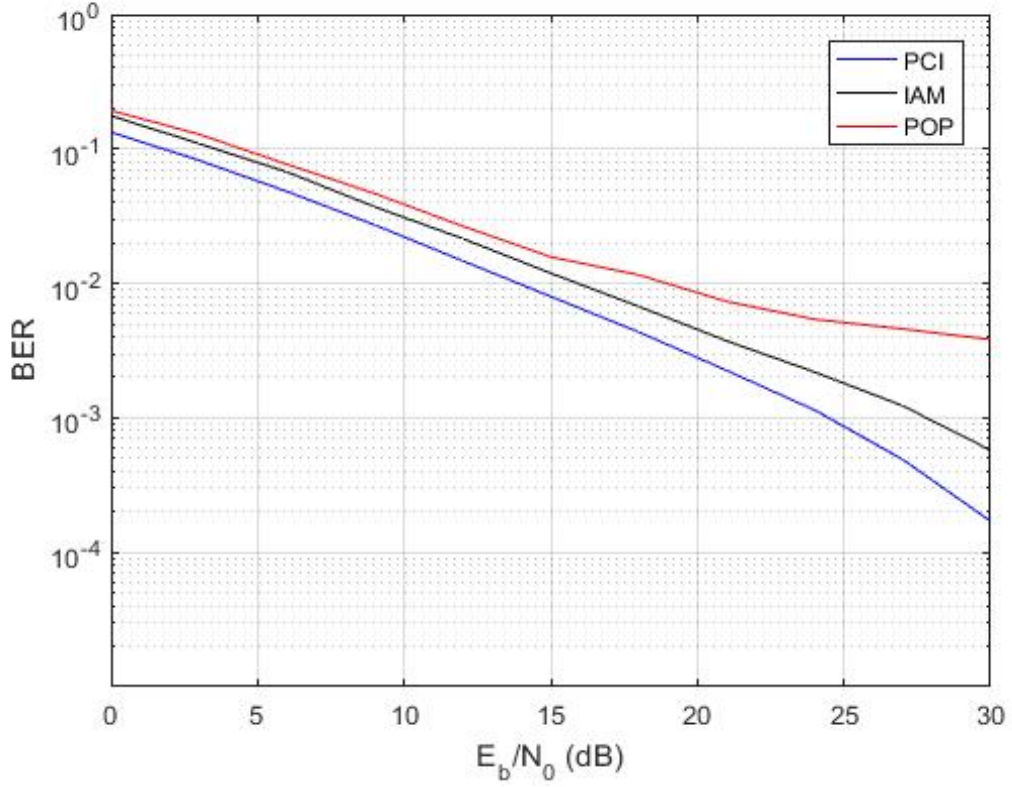


Figure 3.1: MMSE Equalisation with channel estimation (4-QAM, $M=256$, $N=6$)

Conclusion : Though IAM requires preamble of length $3t_0/2$ that is greater than that for POP, it gives improved performance close to $8dB$ at $E_b/N_0 = 30$ than POP. IAM performs better than POP as it accounts for interference from either sides unlike POP which has higher randomness in its handling of term in the denominator of noise.

CHAPTER 4

Carrier Frequency Offset(CFO)

4.1 Effect of CFO on Equalization

The channel model which is given in Eq. 3.1 can be extended to include another one of the effects of multi path transmission i.e carrier frequency offset (CFO).

$$r(t) = (s(t) * h(t, \tau))e^{j2\pi(\epsilon/t_0)t} + \eta(t) \quad (4.1)$$

Here ϵ is the CFO as a fraction of sub-carrier spacing. Here $r(t)$ is sampled at $t_s = t_0/M$ to get $r[n]$. It is then passed through the analysis filter and downsampled by $M/2$. The received signal is given by :

$$\begin{aligned} y_k[n] &= (r[n] * f_k[n])_{\downarrow M/2} \\ &= \sum_{l=0}^{M-1} x_l[n] * ((g_l[m] * h[n, m]e^{j2\pi(\epsilon/M)m}) * f_k[m])_{\downarrow M/2} + \eta_k[n] \end{aligned} \quad (4.2)$$

$$\text{here } \eta_k[n] = (\eta[n] * f_k[n])_{\downarrow M/2}$$

In frequency domain impulse response can be written as :

$$Q_{lk}(e^{j\omega}) = [(G_l(e^{j\omega})H(e^{j\omega})) * \delta(\omega - 2\pi\epsilon)F_k(e^{j\omega})]_{\downarrow M/2} \quad (4.3)$$

It can be seen that multiplication of the transmitted signal by the complex exponential shifts the signal in frequency domain by ϵ/M . The phase rotation between consecutive samples is $2\pi\epsilon/M$ and as we are downsampling by $M/2$, the phase rotation between consecutive received samples is $\pi\epsilon$.

Once we estimate the Carrier frequency offset we have two distortions to take care of. One is the phase rotation itself. The other is the amplitude distortion i.e the shift in the frequency response of the transmitted signal leads to leakage of information from the given sub-carrier and the amplitude response looks as below for CFO = 0.25.

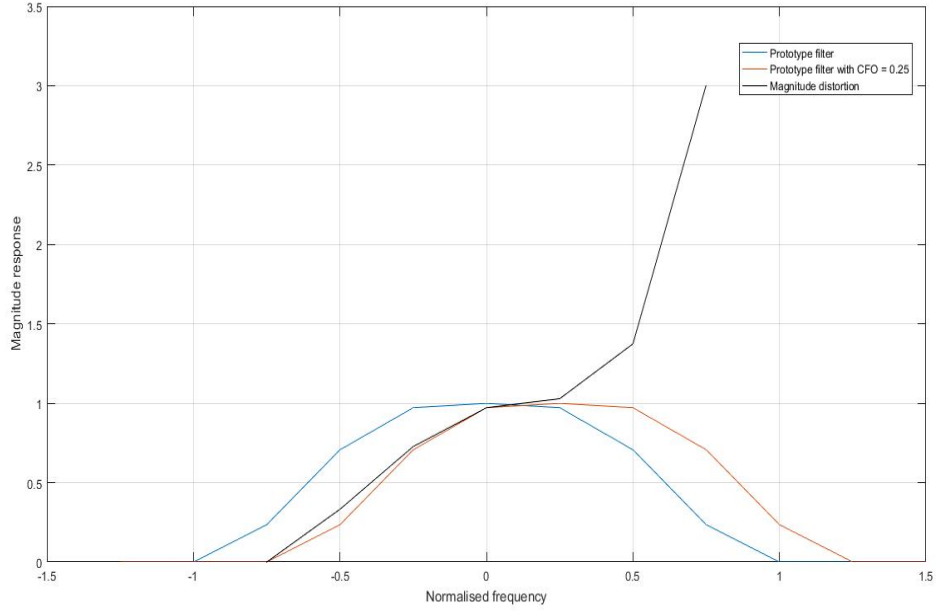


Figure 4.1: Sub-channel frequency response and distortion due to CFO = 0.25

As you can see above the shift in the frequency distorts the synthesis-analysis cascade, to be precise by a factor of $\frac{P(e^{j(2\omega/M + 2\pi\epsilon/M)})}{P(e^{j2\omega/M})}$. Here ω is normalised at sampling rate of the subchannel signal.

4.2 Estimation of CFO

The phase rotation between samples in time caused due to frequency offset is mainly utilised to estimate ϵ . Suppose a pilot at (k, n) is followed by pilot δn samples later then phase rotation $\delta\phi = \pi\epsilon\delta n$ Therefore :

$$\begin{aligned}\epsilon &= \frac{\delta\phi}{\pi\delta n} \\ &= \frac{\angle y'_k[n + \delta n] - \angle y'_k[n]}{\pi\delta n}\end{aligned}\tag{4.4}$$

$$\text{where } y'_k[n] = \theta_{k,n} y_k[n]$$

This estimation can be improved by averaging the CFO determined from different pilots especially when they are separated by same number of samples. We can average the

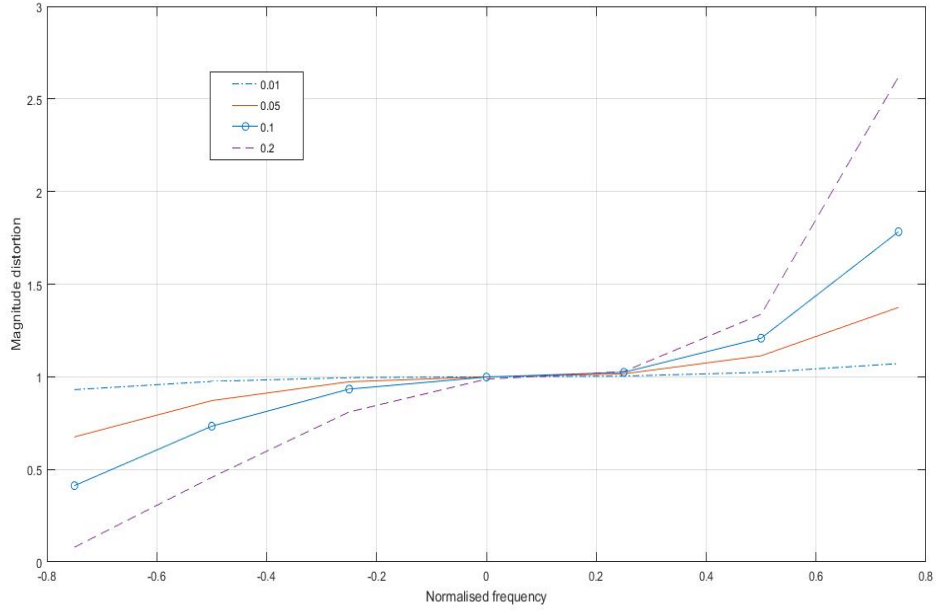


Figure 4.2: Sub-channel frequency response distortion due to CFO = 0.01,0.05,0.1,0.2.

phases weighed in the order of magnitude of data carried over the sub-carriers i.e.,

$$\hat{\epsilon} = \frac{\angle \left(\sum_{(k,n) \in (k_p, n_p)} y'_k[n + \delta n] y_k'^*[n] \right)}{\pi \delta n} \quad (4.5)$$

The preamble for this cfo estimation has a duration of $4t_0$ i.e four multi carrier symbol

$$\text{duration. } x_k[n \frac{M}{2}] = \begin{cases} \pm 1 & \text{if } n \in 0, 4 \text{ and } k \text{ is even} \\ 0 & \text{otherwise} \end{cases}$$

That is, we have two OQAM symbols in preamble distributed over all the sub-carriers separated by $2t_0$ i.e $4(t_0/2)$. So the received symbols are $y_k[0]$ and $y_k[4M/2]$. Since $\theta_k[n + 4] = \theta_k[n]$, we have $y'_k[n + \delta n] y_k'^*[n] = y_k[n + \delta n] y_k^*[n]$ and $\delta n = 4$. To get rid of the adjacent sub-carrier interference we put every alternate sub-carrier to have 0 and to others are put to \pm . So the Eq. 4.5 becomes :

$$\hat{\epsilon} = \frac{\angle \left(\sum_{k'=0}^{M/2-1} y_{2k'}[4(M/2)] y_{2k'}^*[0(M/2)] \right)}{4\pi} \quad (4.6)$$

We face phase ambiguity when $\delta\phi \geq \pi$ i.e when $\epsilon\delta n \geq 1$. It means that the formula given above works only if the CFO $\in [-0.25, 0.25]$. So to mitigate the cases when CFO is higher than 0.25 We take another ϵ reading and this time decrease the δn to 2 aply to

avoid phase ambiguity for higher CFO. Let the reading be $\hat{\epsilon}_1$ and is given by :

$$\hat{\epsilon}_1 = \frac{\angle \left(\sum_{k'=0}^{M/2-1} y_{2k'}[3(M/2)] y_{2k'}^*[1(M/2)] \right)}{2\pi} \quad (4.7)$$

Therefore estimated CFO is given by :

$$\tilde{\epsilon} = \begin{cases} \hat{\epsilon} + 0.5 & \text{if } \hat{\epsilon} > 0.15 \text{ and } \hat{\epsilon}_1 < 0 \\ \hat{\epsilon} - 0.5 & \text{if } \hat{\epsilon} < -0.15 \text{ and } \hat{\epsilon}_1 > 0 \\ \hat{\epsilon} & \text{otherwise} \end{cases}$$

In theory the threshold for $\hat{\epsilon}$ is 0.25. But to make sure that it is estimated correctly with in interval $[-0.25, 0.25]$ even at low SNR we introduce a safety factor of 0.1 for CFO.

4.3 Compensation of CFO

As discussed in section (4.1) phase rotation is one of the distortions due to CFO. Compensation for phase rotation can be carried out by multiplication by a complex exponential : $e^{-j\pi n\epsilon}$. When the offset is moderate, this operation alone guarantees robust communication since amplitude distortion is negligible for values like 0.01, 0.05 as you can see from the Fig. 4.2. But when CFO is higher, frequency shifting alone cannot recover the information leaked into the neighborhood channels.

But with CFO estimated, we can incorporate $\hat{\epsilon}$ into the transmitter-receiver model by modifying the analysis filter as shown in the figure below (replace $e^{-j2\pi l\epsilon/M}$ in the equivalent model by $e^{-j2\pi l\hat{\epsilon}/M}$) to modify the MMSE equaliser coefficients in Eq. 2.9 accordingly. This compensates for the factor $\frac{P(e^{j(2\omega/M+2\pi\epsilon/M)})}{P(e^{j2\omega/M})}$

In absence of multiple pilots, it is difficult to estimate higher CFO's accurately. Also at higher CFO's, with increased interference between adjacent carriers it might not be effective to compensate for each channel separately. Refer Tobias Hidalgo Stitz and Renfors (2009) for more details on CFO compensation and other synchronisation techniques.

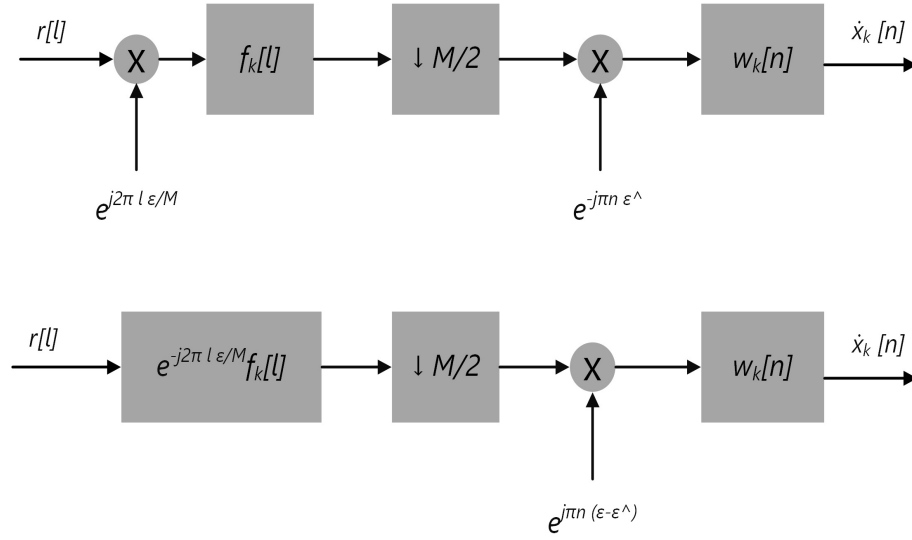


Figure 4.3: Receiver model for sub-channel in presence of CFO with CFO compensation and equalisation showing the actual model and equivalent model for MMSE

4.4 CFO simulations

We estimate the carrier frequency offset with the preamble which is four multicarrier symbols long as described in the section(4.2).The following graph give the maximum and RMS error while estimating CFO at $\frac{E_b}{N_0} = 5, 20, 30$.The estimate is accurate(RMS error) upto order of $10^{-3}, 10^{-4}$ when $\frac{E_b}{N_0} = 5, 20$ respectively.The maximum error as you can see varies as $10^{-2}, 10^{-3}$ to approximately $10^{-3.5}$ as E_b/N_0 varies as 5, 20, 30 respectively.

We compare the BER performance of the MMSE equaliser with and without including the amplitude correction for BER =20, 30.

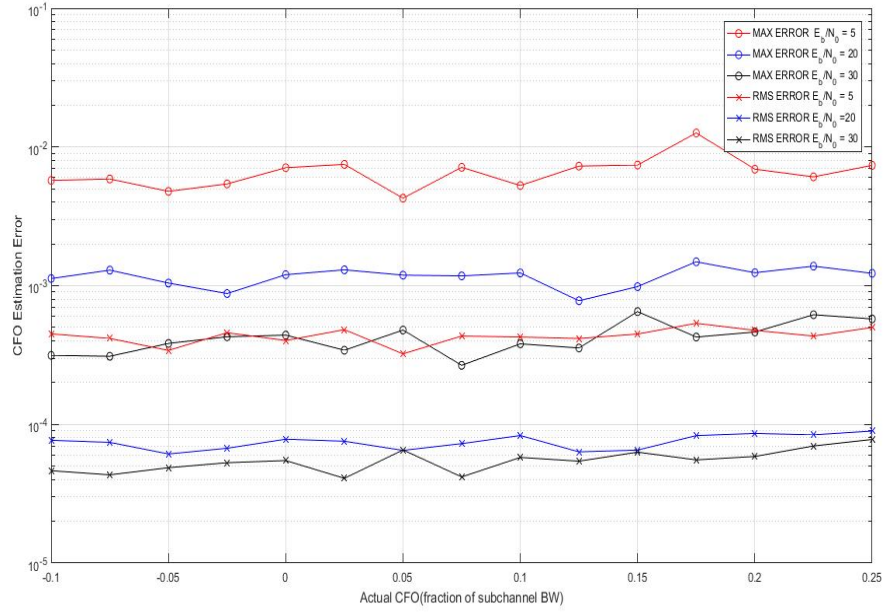


Figure 4.4: MAX error(-o) and RMS error(-x) while estimating CFO for $E_b/N_0 = 5, 20, 30$

Conclusion :

- Though the error in estimating CFO is very low, when $n\epsilon > 1$ the phase rounds up about π and the error $n(\epsilon - \hat{\epsilon})$ becomes significant compared to the rounded off phase after a certain n leading to increase in BER when we estimate CFO.
- With increase in CFO, the estimation error is expected to increase as interference from neighbourhood channels increases. But since the preamble has alternate zeros, it makes interference zero at all data points and so the estimation error stays constant in Fig. 4.4.
- From Fig. 4.5 and Fig. 4.6 you can see that when absolute value of CFO is less than 0.075 and CFO is known perfectly, equaliser performs similarly. So the information leakage into the neighbourhood sub carrier can be considered negligible for such CFO.
- The BER gap between simulations with CFO estimated and perfectly known, drops from 3dB for $E_b/N_0 = 20dB$ to almost 0dB for 30dB. This is a direct result of the greater error in CFO estimation for 20dB as seen from Fig. 4.4

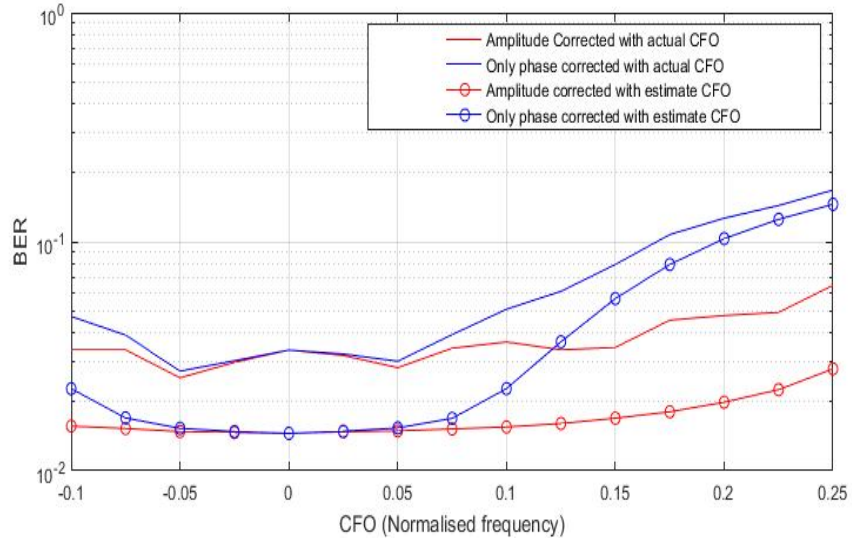


Figure 4.5: BER comparison for $E_b/N_0 = 20$ with CFO estimated and amplitude distortion, phase distortion corrections

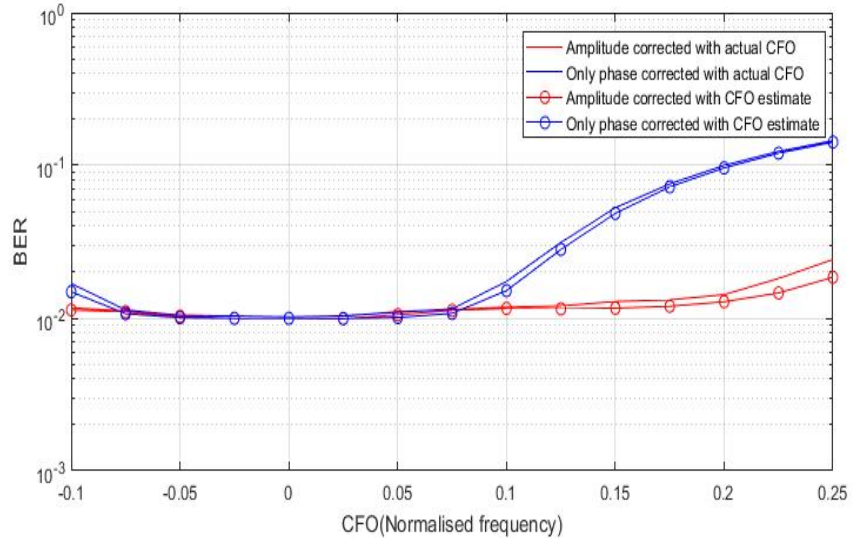


Figure 4.6: BER comparison for $E_b/N_0 = 30$ with CFO estimated and amplitude distortion, phase distortion corrections

REFERENCES

1. **Ari Viholainen, M. H., Maurice Bellanger**, Deliverable 5.1 : Prototype filter and filterbank structure. *In ICT-PHYDYAS project*. 2010.
2. **C.Lele, R. A., J.P.Javaudin and P.Siohan** (2007). Preamble based channel estimation methods for ofdm/oqam over power line.
3. **Dirk S.waldhauser, L. G. and J. A.Nosse** (2008). Mmse subcarreir equalization for filter bank based multicarrier systems. *Institute for Circuit theory and Signal processing, Munich, Germany*.
4. **H.syed, A.**, *Adaptive filters*. John wiley and sons, 2008.
5. **Ikhlef, A. and J. Louveax** (2009). An enhanced mmse per subchannel equaliser for highly frequency selective channels for fbmc/oqam systems. *Communications and Remote sensing Laboratory, EPL, belgium*.
6. **PP.Vaidyanathan**, *Multirate systems and filter banks*. Pearson education -India, 1993.
7. **Qinwei He, A. S.** (2015). Comparision and evaluation of ofdm and fbmc systems. *UMIC Research centre, RWTH Aachen University*.
8. **Tobias hidalgo stitz, A. V., Tero Ihalahein and M. renfors** (2009). Pilot based synchronisation and equalisation in filterbased multicarrier communications.